Imaging morfologico e funzionale

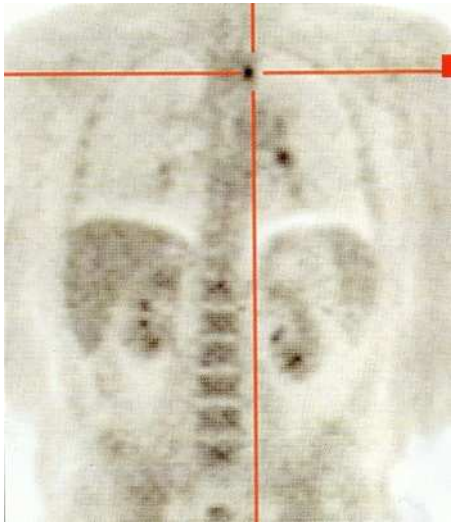

Lo scan PET rivela aree di anormale attività, ma l'esatta localizzazione è sconosciuta

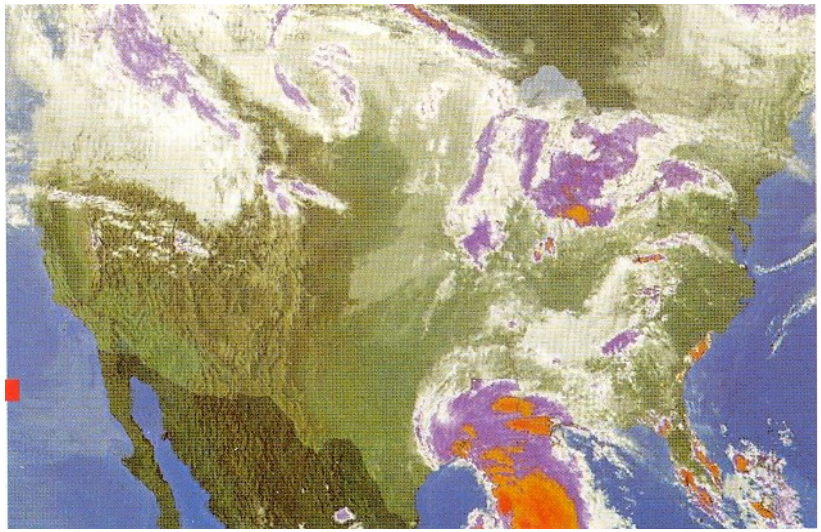

L'immagine dell'atmosfera presa da un satellite mostra le aree di intensa attività ma non le localizza in un preciso contesto geografico

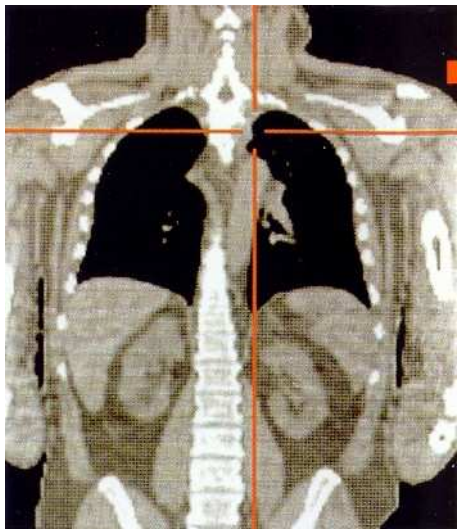

Un'immagine CT mostra precisamente l'anatomia del corpo ma non ne rivela la funzionalità chimica

La mappa mostra i confini degli stati ma non l'attività meteorologica

PET/CT

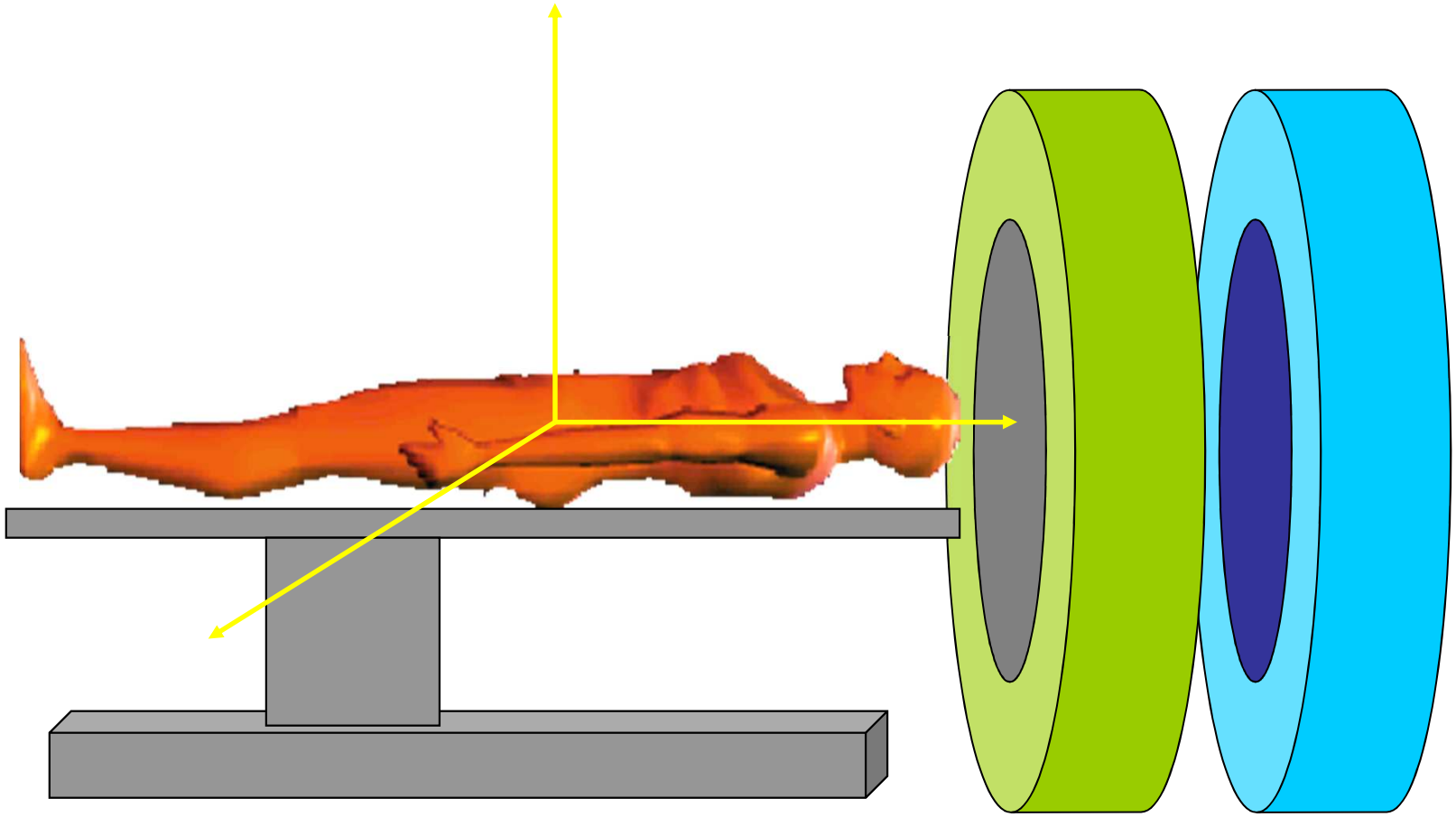

Positron Emission Tomography

La PET in estrema sintesi

Radiofarmaco marcato con nuclide emittente β⁺ somministrato al paziente

Emissione isotropa di β+ che localizza la distribuzione funzionale di radiofarmaco

β+ annichila nel tessuto ⇒ produzione di due fotoni di annichilazione quasi-opposti ($E_\gamma \geq 0.511$ MeV)

Fotoni di annichilazione rivelati in coincidenza elettronica

Ricostruzione della Linea di Volo (LOF) misurata⇒ imaging funzionale

La Reazione di annichilazione

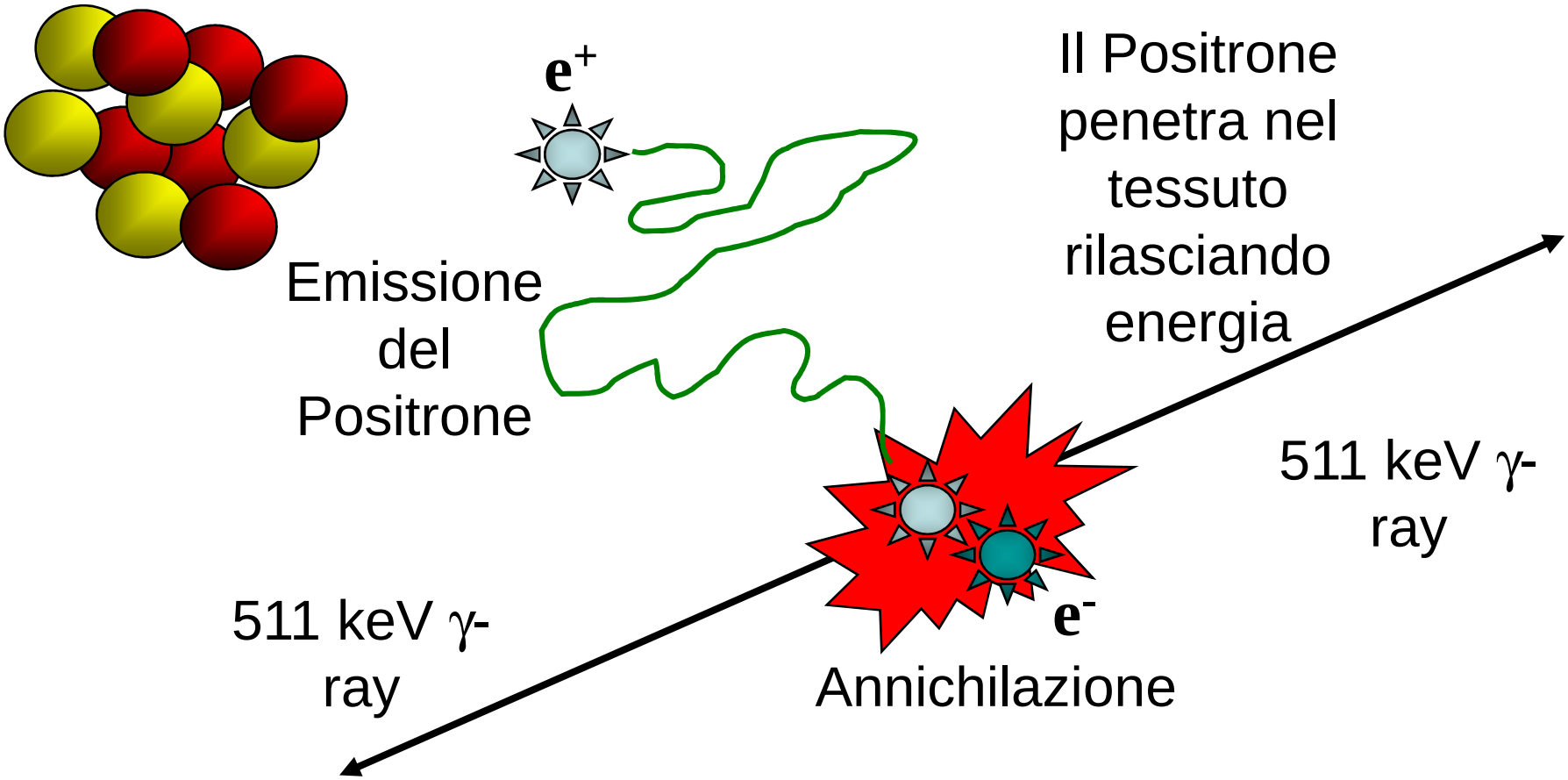

Principio della Tomografia a Emissione di Positroni (PET)

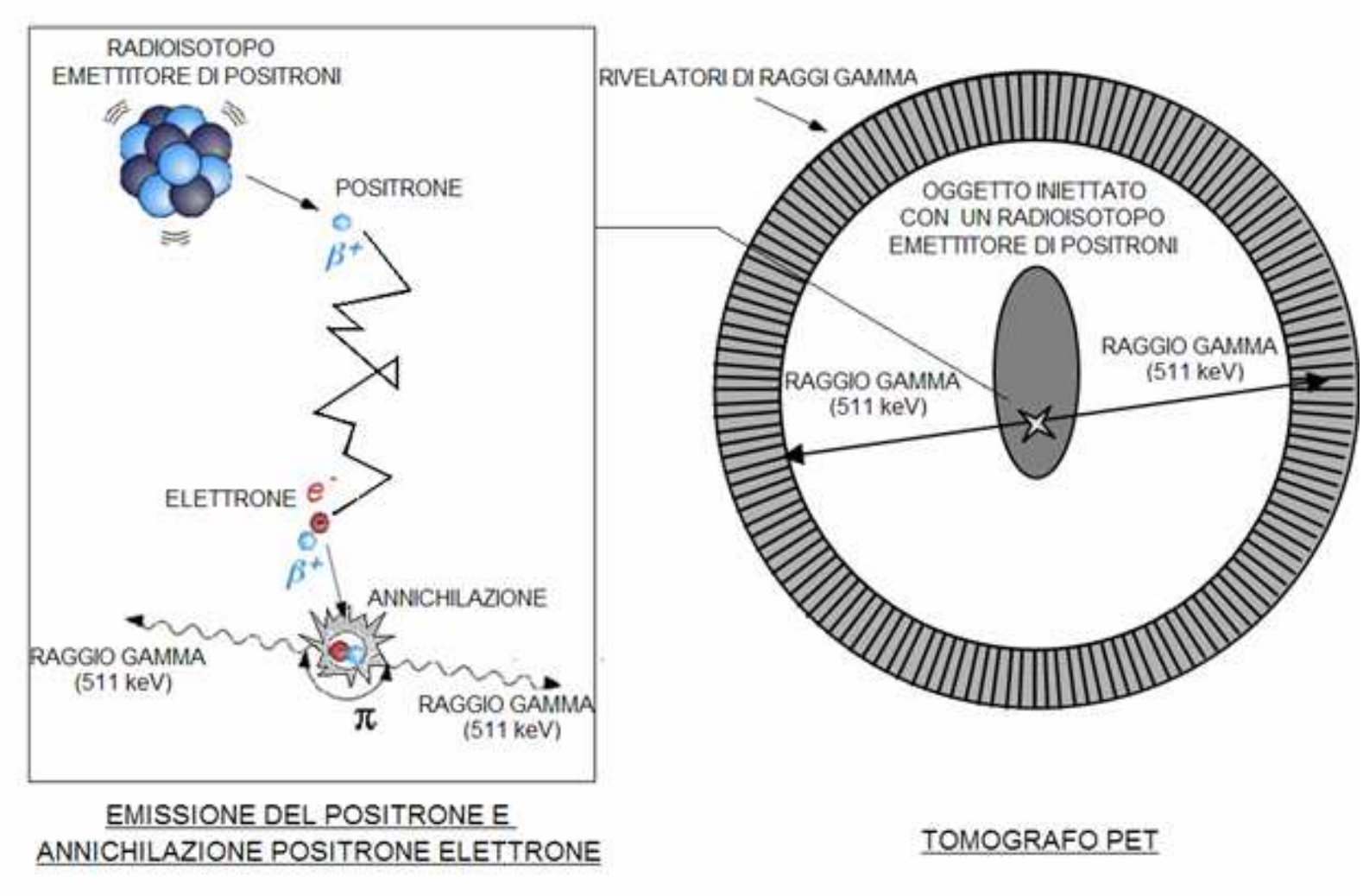

Imaging molecolare

Distribuzione nello spazio e nel tempo di molecole o processi cellulari per lo sviluppo di applicazioni in campo diagnostico o terapeutico.

Thakur & Lentle, 2005

Rappresentazione visuale, caratterizzazione e quantificazione dei processi biologici che avvengono in un essere vivente a livello cellulare e sub-cellulare

In altre parole la misura “in vivo” e caratterizzazione di processi biologici a livello cellulare e molecolare.

Weissleder & Mahmood, 2001

Imaging

I patienti con diagnosi di **carcinoma della prostata** appartengono a due categorie:

1. Pazienti non ancora sottoposti a trattamento con diagnosi istopatologica di malattia e per i quali la stadiazione “remains a challenge”

2. Pazienti con incremento dei valori di prostate-specific antigen (PSA) dopo trattamento, per i quali targeted “**salvage” secondary therapies** possono essere “life-saving” a condizione di riconoscere il/i siti di “recurrence”.

PET Imaging of Prostate Cancer Using Carbon-11-Choline

Toshihiko Hara, Noboru Kosaka and Hiroichi Kishi
Departments of Radiology and Urology, International Medical Center of Japan, Tokyo, Japan

Prostate cancer is difficult to visualize using current techniques. Recently, ^{31}P magnetic resonance spectroscopy has revealed that the tumor, in general, is characterized by an increased uptake of choline into the cell to meet increased synthesis of phosphatidylcholine, an important cell membrane phospholipid. We succeeded in using ^{11}C-choline to visualize prostate cancer and its local metastasis in PET. **Methods:** PET was performed on 10 prostate cancer patients from the level of pelvis to the lower abdomen. After transmission scanning, 370 MBq ^{11}C-choline were injected intravenously. The emission scan was performed 5–15 min postinjection. Finally, PET images were displayed so that each pixel was painted by a specified color representing the degree of the standardized uptake value (SUV). The ^{11}C-choline image was compared with the ^{18}F-fluorodeoxyglucose (FDG) image obtained from the same patient. **Results:** Imaging of prostate cancer and its local metastasis was difficult when ^{18}F-FDG was used because, within the pelvis, the areas of high uptake were concealed by the overwhelmingly abundant radioactivity in urine (in ureters and bladder). By contrast, it was easy when ^{11}C-choline was used because the urinary activity was negligible and tumor uptake was marked. The radioactivity concentration of ^{11}C-choline in prostate cancer and metastatic sites was at an SUV of more than three in most cases. The SUV of ^{18}F-FDG was considerably lower than that of ^{11}C-choline. **Conclusion:** Prostate cancer and its local metastasis were visualized clearly in PET using ^{11}C-choline.

Key Words: PET; carbon-11-choline; prostate cancer

J Nucl Med 1998; 39:990–995

Prostate cancer is a type of cancer in which it is difficult to determine the extent of its invasion and metastasis by current techniques. As a result, it also is difficult to estimate the outcome of surgery, radiotherapy, chemotherapy and hormonal therapy.

Despite the effectiveness of ^{18}F-fluorodeoxyglucose (FDG) PET in imaging various tumors, this technique is not appropriate for prostate cancer detection because the urinary excretion of ^{18}F-FDG is so large that it interferes with the imaging of tumors in the pelvis.

Recently, ^{31}P magnetic resonance spectroscopy (MRS) in vivo and in vitro has revealed an elevated level of phosphatidylcholine in tumors, which is the most abundant phospholipid in the cell membranes of all eukaryotic cells (*1–8*). It is thought that this elevation is the result of increased uptake of choline, a precursor of the biosynthesis of phosphatidylcholine (*9–14*).

We previously reported an application of ^{11}C-labeled choline for imaging brain tumors using PET (*15*). Since then, we successfully used this tracer to image many other types of tumors (*16*). Urinary excretion is negligible with ^{11}C-choline. Here we report the effectiveness of this tracer in PET imaging of prostate cancer in patients.

The tissue uptake of ^{11}C-choline is rapid after the intravenous injection, in accord with the rapid blood clearance (*15*). Once the radioactivity is absorbed into the tissue, the tissue uptake does not change for a long time with decay correction. It is practically constant from 5 to 40 min after injection in most organs. Because of these characteristics, the entire procedure of ^{11}C-choline PET in one patient takes 40 min.

Received Feb. 1, 1997; revision accepted Oct. 9, 1997.
For correspondence or reprints contact: Toshihiko Hara, MD, Department of Radiology, International Medical Center of Japan, 1-21-1 Toyama, Shinjuku-ku, Tokyo 162, Japan.

MATERIALS AND METHODS

Patients

With our ethics committee's approval and the patients' informed consent, 10 patients who were admitted to the urology department of our hospital participated in this study. They had both ^{11}C-choline PET and ^{18}F-FDG PET studies before the beginning of treatment (two patients were reexamined after treatment, as discussed later). The PET studies were performed over 2 days before noon while patients were in the fasting state. Histological diagnosis was obtained on all patients before the PET study.

Radiopharmaceutical

Carbon-11-choline was prepared according to the method reported previously (*15*). Briefly, using a cyclotron to produce ^{11}C, and after reacting ^{11}C-methyl iodide with "neat" dimethylaminoethanol at 120°C for 5 min, the resulting product, ^{11}C-choline, was purified by evaporation of unreacted substrates followed by treatment of the remaining substance with cation-exchange resin (−COOH form), yielding an injection solution dissolved in saline. All synthetic and purification procedures were performed in an automated apparatus (Japan Steel Works, Muroran, Hokkaido, Japan).

Imaging Protocol

PET images were obtained using a PET camera (Headtome IV, 6-mm spatial resolution, Shimadzu, Kyoto, Japan) equipped with three rings to produce five slices at 13-mm intervals. For ^{11}C-choline, after acquiring transmission data, 370 MBq ^{11}C-choline were injected. Five minutes later, the emission scan was started. For ^{18}F-FDG, after acquiring transmission data followed by injection of 370 MBq ^{18}F-FDG, the patient was allowed to void. After placing the patient in the fixed bed position, the emission scan was started 40 min after injection. During transmission and emission scanning, the bed position was shifted six times upward from the level of pelvis to that of liver, with a total data acquisition time of 18 min. PET images were reconstructed after correcting the emission data by the transmission data. The horizontal images were displayed sequentially on a computer screen, where their slice levels were shown in a planar image made up from a whole set of the horizontal images (The planar image was helpful in determining the position of the prostate.) Finally, the horizontal images were displayed on the screen using a scale of the standardized uptake value (SUV). SUV is defined as:

$$\text{SUV} = \frac{\text{Regional radioactivity concentration}}{\text{Total injected dose/body weight}},$$

where the radioactivity concentration in a pixel (Bq/ml) was to be determined from an apparent pixel count (cps/pixel volume) and a

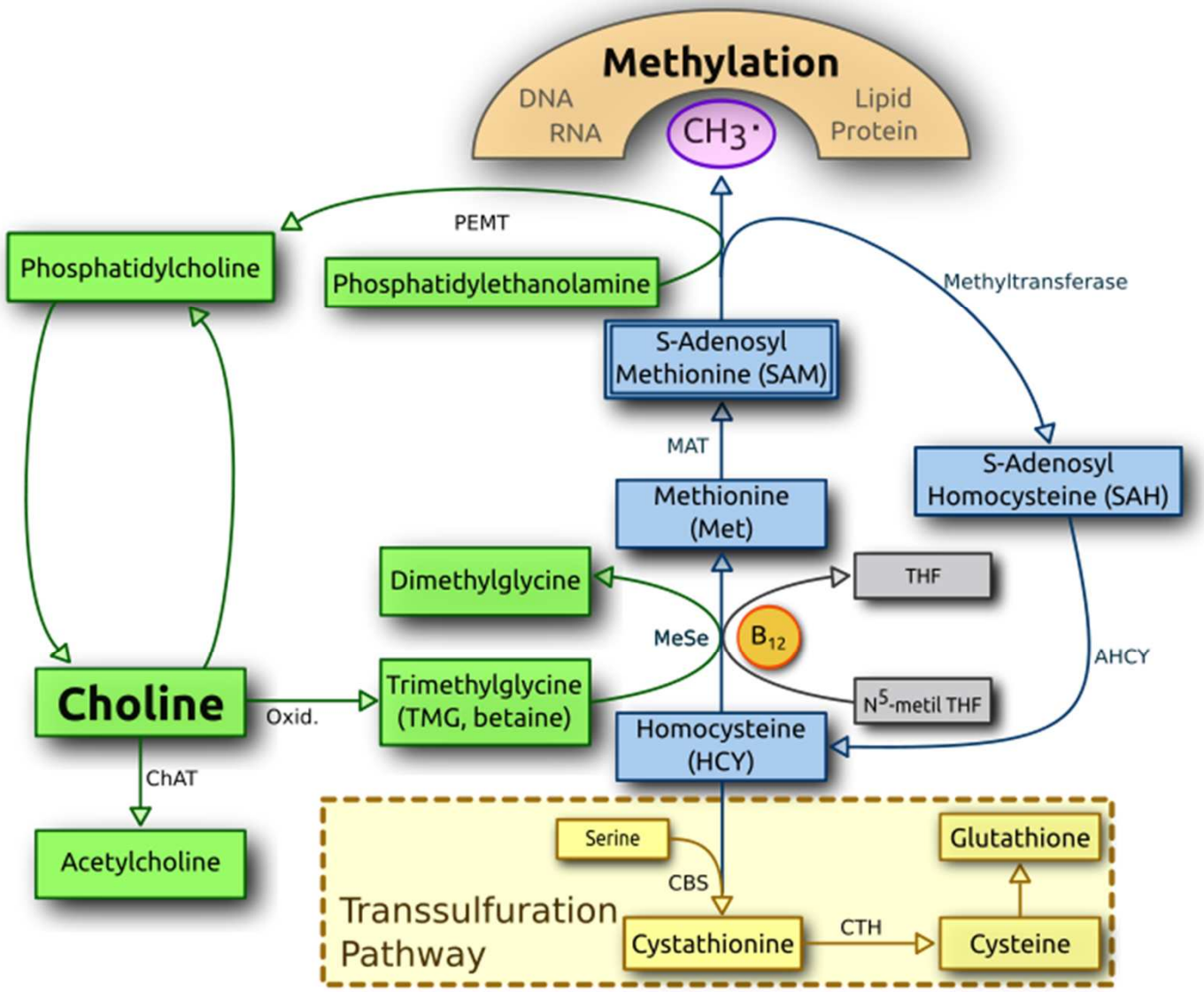

Choline and its metabolites are needed for three main physiological purposes: structural integrity and signaling roles for cell membranes, cholinergic neurotransmission (acetylcholine synthesis), and a major source for methyl groups via its metabolite, trimethylglycine (betaine), which participates in the S-adenosylmethionine (SAMe) synthesis pathways.[

Modello “ Ball-and-stick” della **colina**, catione idrosolubile, nutriente essenziale.

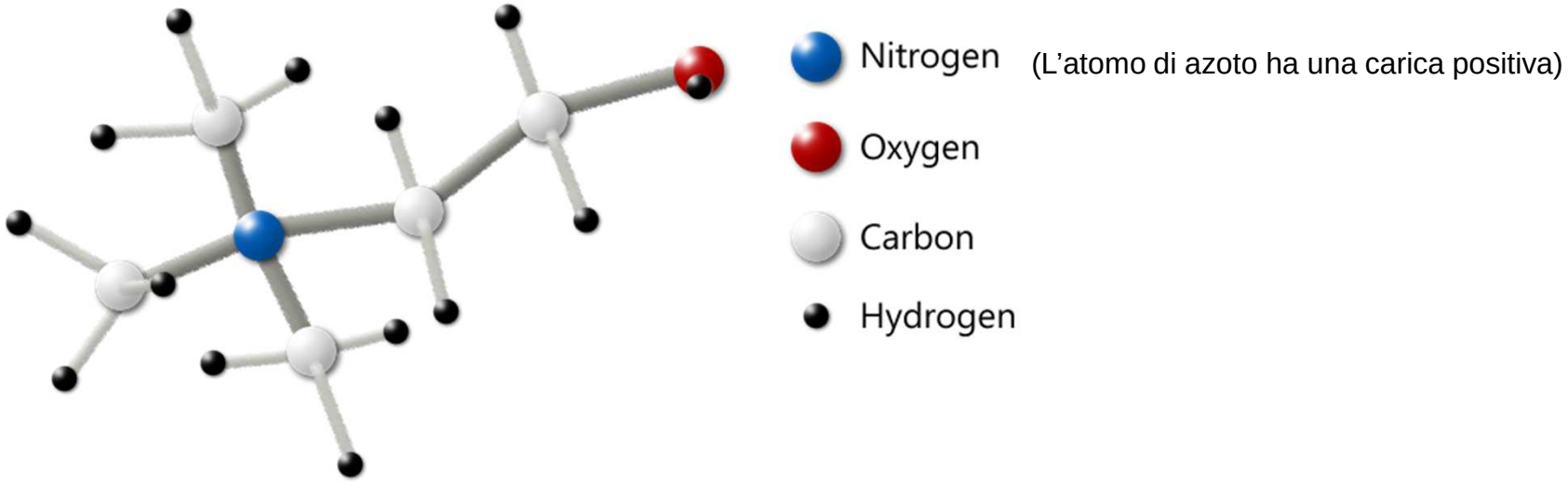

(L’atomo di azoto ha una carica positiva)

Choline is a quaternary ammonium salt with the chemical formula (CH3)3N+(CH2)2OHX−, where X− is a counter-ion such as chloride, hydroxide or tartrate. Choline chloride can form a low-melting deep eutectic solvent mixture with urea with unusual properties. **The** salicylate salt is used topically for pain relief of aphthous ulcers.

PET/CT – Colina

In sintesi:

•Il processo biochimico alla base dell'uso della Colina come tracciante PET è la **sintesi delle membrane**.

•Tutte le cellule usano **colina come precursore per la biosintesi di fosfolipidi**, componenti essenziali delle membrane cellulari.

•La colina entra nella cellula utilizzando **trasportatori specifici** di membrana

•All'interno della cellula la colina è fosforilata attraverso l'azione dell'enzima colina-chinasi (CK).

•La fosforil-colina è ulteriormente metabolizzata in fosfatidil-colina (**lecitina**), principale fosfolipide di membrana.

Le **cellule tumorali**, necessitano di quantitativi elevati di colina nei processi replicativi/proliferativi.

PET/CT – Colina

•Considering the known limitations of the current imaging modalities, many investigations have assessed the value of **^{11}C- and ^{18}F-choline** PET/CT as a **single noninvasive modality in the restaging of prostate cancer patients with biochemical recurrence** after initial treatment.

•A **sensitivity of between 43% and 95% was reported** using choline PET/CT in the detection of malignant lesions in recurrent prostate cancer. Moreover, several studies have evaluated the influence of various clinical (e.g., **tumor stage, Gleason score, and ADT**) and laboratory findings (e.g., **PSA level, PSA velocity, and PSA doubling time**) on choline PET/CT in patients with rising PSA levels after initial treatment.

PET/CT – …oltre la Colina

Novel Tracers and Their Development for the Imaging of Metastatic Prostate Cancer*

Andrea B. Apolo[1,2], Neeta Pandit-Taskar[3,4], and Michael J. Morris[1,2]

[1]Genitourinary Oncology Service, Department of Medicine, Memorial Sloan-Kettering Cancer Center, New York, New York; [2]Department of Medicine, Weill Medical College of Cornell University, New York, New York; [3]Nuclear Medicine Service, Department of Radiology, Memorial Sloan-Kettering Cancer Center, New York, New York; and [4]Department of Radiology, Weill Medical College of Cornell University, New York, New York

There are presently no accurate methods of imaging prostate cancer metastases to bone. An unprecedented number of novel imaging agents, based on the biology of the disease, are now available for testing. We reviewed contemporary molecular imaging modalities that have been tested in humans with metastatic prostate cancer, with consideration of the studies' adherence to current prostate cancer clinical trial designs. Articles from the years 2002 to 2008 on PET using ^{18}F-FDG, ^{11}C-choline, ^{18}F-choline, ^{18}F-flouride, ^{11}C-acetate, ^{11}C-methionine, and ^{18}F-fluoro-5α-dihydrotestosterone in patients with metastatic prostate cancer were reviewed. Although these studies are encouraging, most focus on the rising population with prostate-specific antigen, and many involve small numbers of patients and do not adhere to consensus criteria for clinical trial designs in prostate cancer. Hence, although many promising agents are available for testing, such studies would benefit from closer collaboration between those in the fields of medical oncology and nuclear medicine.

Key Words: prostate cancer; positron emission tomography; ^{18}F-fluorodeoxyglucose; ^{11}C-choline; ^{18}F-fluorocholine; ^{11}C-acetate; ^{11}C-methionine; ^{18}F-fluoro-5α-dihydrotestosterone

J Nucl Med 2008; 49:2031–2041
DOI: 10.2967/jnumed.108.050658

In the past several decades, understanding of the molecular biology of prostate cancer has expanded, particularly related to growth despite androgen-reducing agents and the transformation from a tumor cell dependent on prostate stroma to one that participates in bone metabolism (*1,2*). The identification of biologic targets not only has led to the introduction of novel therapies for prostate cancer but also has opened up new possibilities for imaging the disease. These biologic targets can be used to characterize underlying molecular biology of the tumor at a lesional level, assess the pharmacodynamics of targeted therapy, and assess clinical responses.

Such new imaging modalities are sorely needed for prostate cancer patients, particularly those with metastatic disease. Between 80% and 90% of prostate cancer patients with metastatic disease have involvement of the axial skeleton (*3–6*). Although contemporary data show an increasing proportion of soft-tissue lesions in prostate cancer patients with metastatic disease (*4,5*), bone metastases still continue to represent the predominant manifestation for most patients and the primary cause of morbidity and mortality. However, bone metastases are considered nonmeasurable by the Response Evaluation Criteria in Solid Tumors. The lack of accurate imaging modalities to directly, reproducibly, and effectively delineate bone metastases limits the clinical management of prostate cancer patients and the advancement of new therapies.

It is difficult to introduce and test any new agent in prostate cancer—whether it is a therapeutic drug or a novel tracer—because there is no gold standard imaging modality that can establish whether a drug is having an effect on the cancer, whether a tracer is actually detecting disease, or whether there has been a change in disease. As a result, designing clinical trials for prostate cancer is uniquely challenging (*7,8*). In addition to the difficulty of imaging prostate cancer, the disease itself has a heterogeneous clinical course, as do its patients, who face significant noncancer-related morbidities as well.

Faced with these challenges, the field has adopted a clinical-states framework for organizing the natural history of disease (Fig. 1). The model highlights the objectives of the intervention rather than the treatment itself. In addition, unlike traditional staging schema based on primary tumor characteristics, nodal status, and metastatic involvement at diagnosis, the model is not fixed but describes the entire disease course.

Leaders in prostate cancer clinical trials have developed state-specific consensus criteria for clinical trials, from eligibility criteria to outcome measures (*9–11*). These

Received Aug. 9, 2008; revision accepted Oct. 6, 2008.
For correspondence or reprints contact: Michael J. Morris, Genitourinary Oncology Service, 1275 York Ave., New York, NY 10065.
E-mail: morrism@mskcc.org
*NOTE: FOR CE CREDIT, YOU CAN ACCESS THIS ACTIVITY THROUGH THE SNM WEB SITE (http://www.snm.org/ce_online) THROUGH DECEMBER 2009.
No potential conflict of interest relevant to this article was reported.

New Agents and Techniques for Imaging Prostate Cancer

Atif Zaheer, Steve Y. Cho, and Martin G. Pomper

Russell H. Morgan Department of Radiology and Radiological Science, Johns Hopkins Medical Institutions, Baltimore, Maryland

The successful management of prostate cancer requires early detection, appropriate risk assessment, and optimum treatment. An unmet goal of prostate cancer imaging is to differentiate indolent from aggressive tumors, as treatment may vary for different grades of the disease. Different modalities have been tested to diagnose, stage, and monitor prostate cancer during therapy. This review briefly describes the key clinical issues in prostate cancer imaging and therapy and summarizes the various new imaging modalities and agents in use and on the horizon.

Key Words: molecular imaging; MRI; PET; SPECT; radiopharmaceutical

J Nucl Med 2009; 50:1387–1390
DOI: 10.2967/jnumed.109.061838

Prostate cancer (PCa) is the most common malignancy among men in the United States, with mortality superseded only by lung cancer, accounting for 10% of all cancer-related deaths in 2008 (*1*). PCa is currently characterized by its TNM stage, Gleason score, and prostate-specific antigen (PSA) serum level. PSA testing is the mainstay of detection and has reduced the rate of death from PCa. However, there remains growing concern regarding the potential risk of overdiagnosis and, consequently, overtreatment of potentially indolent disease. The rate of overdiagnosis of PCa, defined as diagnosis in men who would not have clinical symptoms during their lifetime, has been estimated to be as high as 50% (*2*). Urinary incontinence and erectile dysfunction are not uncommon after radical prostatectomy. Although PSA is a good marker for assessing response to therapy and detecting recurrence, PSA lacks the ability to differentiate low-grade from high-grade cancers. New biomarkers such as the recently described stage-dependent urinary marker sarcosine (*3*) may soon rival PSA for monitoring the presence and extent of disease.

Conventional imaging, which includes CT, MRI, and ultrasound, is currently used to detect organ-confined or metastatic disease for staging and determining prognosis. However, there is substantial room for improvement in the use of imaging for determining tumor grade and for identifying minimal, metastatic disease. At a recent workshop, the National Cancer Institute proposed intervention for PCa at 4 different levels (*4*). The roles of imaging in initial diagnosis, staging, disease recurrence after treatment, and assessment of response to therapy were discussed. Also discussed were the multiple new molecular imaging agents that are being tested and can be incorporated into the current paradigm of diagnosis, treatment, and rapid detection of recurrent disease. We will address new approaches to imaging PCa in the context of these 4 levels of intervention.

Received Mar. 27, 2009; revision accepted Jun. 29, 2009.
For correspondence or reprints contact: Martin G. Pomper, Johns Hopkins Medical Institutions, 1550 Orleans St., 492 CRB II, Baltimore, MD 21231.
E-mail: mpomper@jhmi.edu

INITIAL DIAGNOSIS

The current standard for diagnosis of PCa is sextant biopsy guided by transrectal ultrasound. PCa is the only malignancy for which the diagnosis is made from tissue obtained on a blind biopsy. That technique tends to underestimate the histologic grade. The heterogeneous nature and multifocality of the tumor renders a blind biopsy inadequate in assessing tumor grade. Up to 28% of clinically significant cancers have been reported to go undetected by the traditional sextant biopsy method (*5*). Imaging data, which are not susceptible to the sampling error that accompanies biopsy, can enhance biopsy by allowing for a more targeted approach.

T2-weighted MRI provides higher spatial and contrast resolution than does transrectal ultrasound and CT but lacks specificity (*6*). Magnetic resonance spectroscopy (MRS) provides a noninvasive method of detecting low-molecular-weight biomarkers within the cytosol and extracellular spaces of the prostate. MRS relies on the loss of a normal citrate peak from the peripheral zone and an increase in the choline peak, an indirect marker of cell death. The ratio of (choline + creatine)/citrate in PCa exceeds the mean ratio found in healthy prostate tissue. Pulsed field gradients are generally used for localization using volumes of interest and include point-resolved spectroscopy and stimulated echo acquisition mode, summarized in an excellent review by Mueller-Lisse and Scherr (*7*). Although the addition of MRS to MRI alone does not significantly improve the accuracy of PCa detection, together they are more accurate than biopsy in certain regions of the prostate, such as the apex (*8*). MRS combined with MRI may also supplement standard biopsy guided by endorectal ultrasound (*9*). Measurement of prostate tumor (choline + creatine)/citrate and tumor volume by MRS imaging correlates with Gleason score (*10*). In a small clinical trial, improved spatial and spectral resolution were achieved at 7 T, allowing for more sensitive detection of spermine, a metabolite having an inverse correlation with the presence of tumor cells (*11*).

Despite the limited ability of ultrasound to delineate cancer, ultrasound has the advantage of low cost, wide availability, and speed over MR image–guided interventions. A recent study demonstrated the feasibility of prostate biopsy guided by fusion of transrectal ultrasound and MRI, with the entire procedure, including fusion, requiring about 10 min (*12*). Furthermore, with an ultrasound 3-dimensional (3D) navigation system, such as that developed by Bax et al. (*13*), needle guidance can be used for sampling small lesions. Tests of the accuracy of biopsy needle guidance in agar prostate phantoms showed a mean error of 1.8 mm in the 3D location of the biopsy core, with less than 5% error in volume estimation.

Published in final edited form as:
Curr Med Chem. 2012 ; 19(6): 856–870.

Glutamate Carboxypeptidase II in Diagnosis and Treatment of Neurologic Disorders and Prostate Cancer

C. Bařinka[1,*], **C. Rojas**[2], **B. Slusher**[2], and **M. Pomper**[3]

[1]Institute of Biotechnology, Academy of Sciences of the Czech Republic, Videnska 1083, 14200 Praha 4, Czech Republic

[2]Johns Hopkins Brain Science Institute, Neuro Translational Drug Discovery Program, 855 North Wolfe Street, Baltimore, MD 21205, USA

[3]Russell H. Morgan Department of Radiology and Radiological Sciences, Johns Hopkins Medical Institutions, 1550 Orleans Street, Baltimore, MD 21231, USA

Abstract

Glutamate carboxypeptidase II (GCPII) is a membrane-bound binuclear zinc metallopeptidase with the highest expression levels found in the nervous and prostatic tissue. Throughout the nervous system, glia-bound GCPII is intimately involved in the neuron-neuron and neuron-glia signaling *via* the hydrolysis of N-acetylaspartylglutamate (NAAG), the most abundant mammalian peptidic neurotransmitter. The inhibition of the GCPII-controlled NAAG catabolism has been shown to attenuate neurotoxicity associated with enhanced glutamate transmission and GCPII-specific inhibitors demonstrate efficacy in multiple preclinical models including traumatic brain injury, stroke, neuropathic and inflammatory pain, amyotrophic lateral sclerosis, and schizophrenia. The second major area of pharmacological interventions targeting GCPII focuses on prostate carcinoma; GCPII expression levels are highly increased in androgen-independent and metastatic disease. Consequently, the enzyme serves as a potential target for imaging and therapy. This review offers a summary of GCPII structure, physiological functions in healthy tissues, and its association with various pathologies. The review also outlines the development of GCPII-specific small-molecule compounds and their use in preclinical and clinical settings.

Keywords

Metalloprotease; prostate-specific membrane antigen; glutamate excitotoxicity; prostate cancer; N-acetylaspartylglutamate

1. INTRODUCTION

Glutamate carboxypetidase II (GCPII; EC 3.4.17.21) also known as prostate specific membrane antigen (PSMA), N-acetylated-alpha-linked acidic dipeptidase (NAALADase), and folate hydrolase (FOLH1) is a zinc-dependent peptidase that is increasingly recognized as a target of therapeutic interventions in a variety of neurologic disorders as well as a marker for imaging of and therapy for prostate cancer (PCa). GCPII was identified by different laboratories in different tissues of different species more than 20 years ago; original designations reflected the belief that the identified protein was either a unique entity in a

*Address correspondence to this author at the Institute of Biotechnology AS CR, v.v.i., Laboratory of Structural Biology, Videnska 1083, 14200 Praha 4, Czech Republic; Tel: +420-296-443-615; Fax: +420-296-443-610; cyril.barinka@img.cas.cz.

PSMA

Glutamate carboxypeptidase II (GCPII), also known as N-acetyl-L-aspartyl-L-glutamate peptidase I (NAALADase I), NAAG peptidase, or **prostate-specific membrane antigen (PSMA)** is an enzyme that in humans is encoded by the *FOLH1* (folate hydrolase 1) gene.[1] Human GCPII contains 750 amino acids and weighs approximately 84 kDa.[2]

GCPII is a zinc metalloenzyme that resides in membranes. Most of the enzyme resides in the extracellular space.

GCPII is a class II membrane glycoprotein. It catalyzes the hydrolysis of N-acetylaspartylglutamate (NAAG) to glutamate and N-acetylaspartate (NAA).

Neuroscientists primarily use the term NAALADase in their studies, while those studying folate metabolism use folate hydrolase, and those studying prostate cancer or oncology, PSMA.
All of which refer to the same protein glutamate carboxypeptidase II.

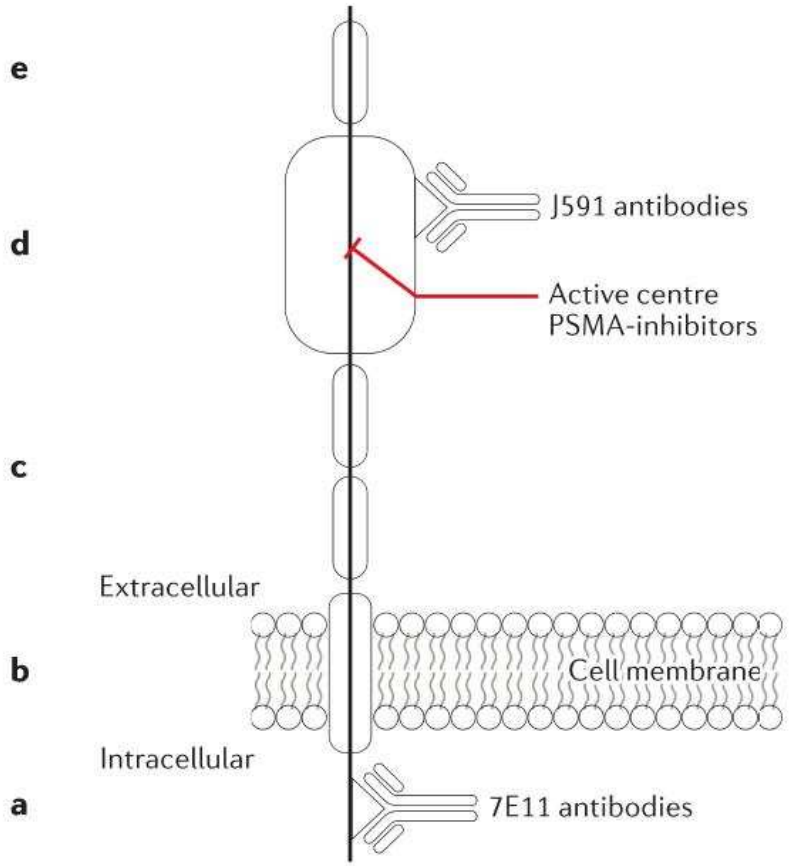

Figure 1 | **The structure of prostate-specific membrane antigen (PSMA), its binding sites for PSMA ligands and the most frequently used antibodies. a** | The short intracellular domain containing a binding site that can be targeted with 7E11 antibodies. **b** | The hydrophobic transmembrane region. The extracellular part of PSMA consists of section **c** | that contains two domains of unknown function and proline-rich and glycine-rich regions as linkers, **d** | that is the large catalytic domain, which contains a binding site for J591 antibodies as well as the active substrate recognition site that is being targeting by PSMA inhibitors and **e** | the final domain of unknown function to which a helical dimerization domain is localized.

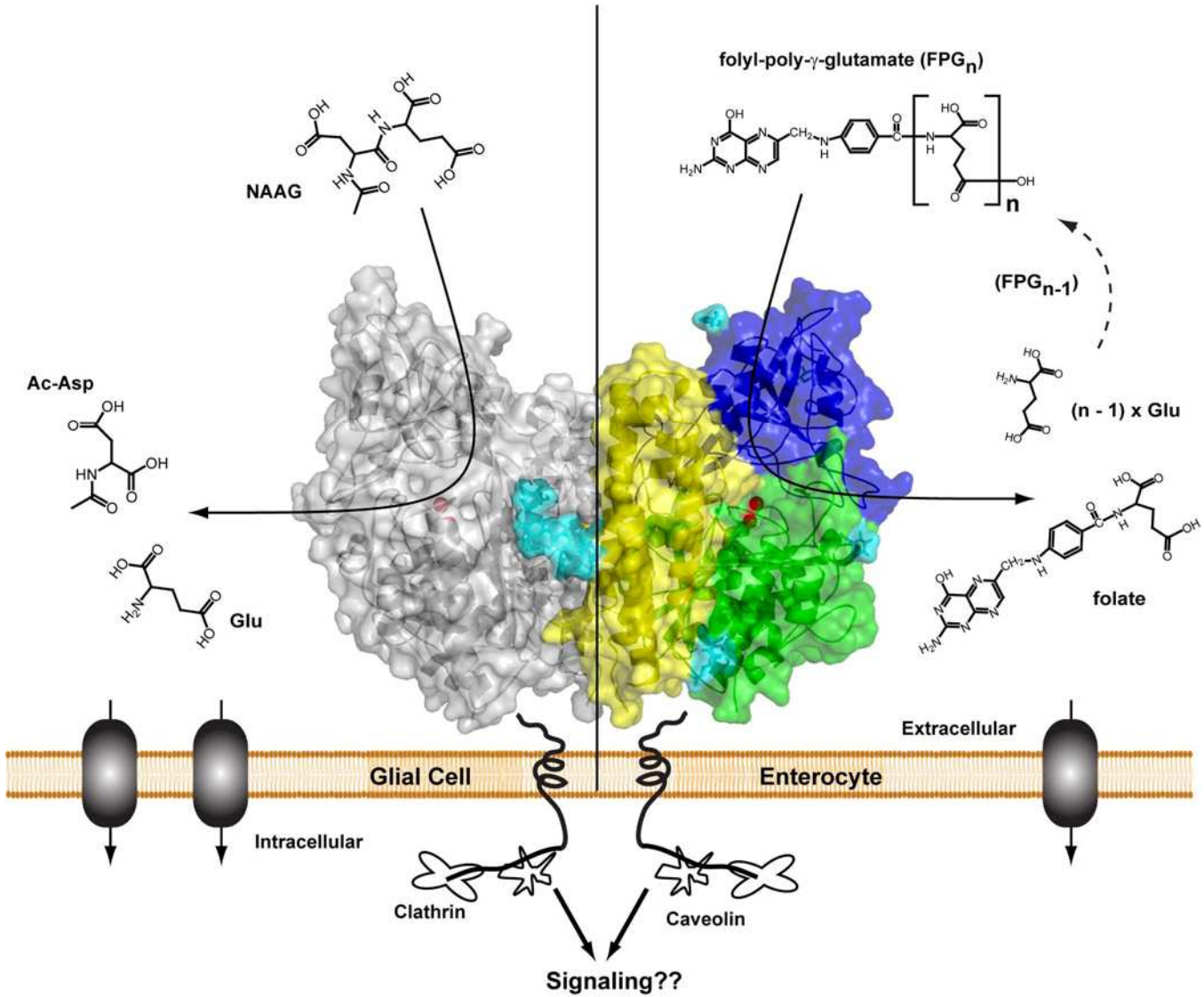
NERVOUS SYSTEM
SMALL INTESTINE
folyl-poly-γ-glutamate (FPG$_n$)
NAAG
(FPG$_{n-1}$)
(n - 1) x Glu
Ac-Asp
Glu
folate
Extracellular
Glial Cell
Enterocyte
Intracellular
Clathrin
Caveolin
Signaling??

PSMA

L’espressione di PSMA è notevolmente aumentata nel tumore della prostata, approssimativamente 100 volte rispetto ai tessuti normali.
In alcuni tumori della prostata, PSMA è il secondo prodotto genico “upregulated”, con un **aumento di 8- 12- volte** rispetto alle cellule prostatiche non carcinomatose.

Nel tumore della prostata l **tumori a più alta espressione** sono associati a più veloce progressione di malattia e più alta percentuale di recidive.

Studi in vitro con linee cellulari di tumore mammario e della prostata a **diminuita espressione di PSMA** mostrano significativa riduzione della proliferazione, migrazione, invasione, adesione e sopravvivenza cellulare.

PSMA PET nella recente letteratura

«PSMA PET PROSTATE»

Nel corso del 2016 risultano pubblicati 55 lavori (full papers e review)

Eur J Nucl Med Mol Imaging (2013) 40:486–495
DOI 10.1007/s00259-012-2298-2

ORIGINAL ARTICLE

PET imaging with a [^{68}Ga]gallium-labelled PSMA ligand for the diagnosis of prostate cancer: biodistribution in humans and first evaluation of tumour lesions

A. Afshar-Oromieh · A. Malcher · M. Eder · M. Eisenhut · H. G. Linhart · B. A. Hadaschik · T. Holland-Letz · F. L. Giesel · C. Kratochwil · S. Haufe · U. Haberkorn · C. M. Zechmann

Received: 21 August 2012 / Accepted: 6 November 2012 / Published online: 24 November 2012

Abstract
Purpose Prostate-specific membrane antigen (PSMA) is a cell surface protein with high expression in prostate carcinoma (PC) cells. Recently, procedures have been developed to label PSMA ligands with ^{68}Ga, ^{99m}Tc and $^{123/124/131}$I. Our initial experience with Glu-NH-CO-NH-Lys-(Ahx)-[^{68}Ga(HBED-CC)](^{68}Ga-PSMA) suggests that this novel tracer can detect PC relapses and metastases with high contrast. The aim of this study was to investigate its biodistribution in normal tissues and tumour lesions.
Methods A total of 37 patients with PC and rising prostate-specific antigen (PSA) levels were subjected to ^{68}Ga-PSMA positron emission tomography (PET)/CT. Quantitative assessment of tracer uptake was performed 1 and 3 h post-injection (p.i.) by analysis of mean and maximum standardized uptake values ($SUV_{mean/max}$) of several organs and 65

A. Afshar-Oromieh (✉) · A. Malcher · F. L. Giesel · C. Kratochwil · S. Haufe · U. Haberkorn · C. M. Zechmann
Department of Nuclear Medicine, University Hospital of Heidelberg, Im Neuenheimer Feld 400,
69120 Heidelberg, Germany
e-mail: a.afshar@gmx.de

A. Malcher
e-mail: anna.malcher@gmx.de

F. L. Giesel
e-mail: f.giesel@dkfz.de

C. Kratochwil
e-mail: clemens.kratochwil@t-online.de

S. Haufe
e-mail: sabine.haufe@med.uni-heidelberg.de

U. Haberkorn
e-mail: uwe.haberkorn@med.uni-heidelberg.de

C. M. Zechmann
e-mail: christian.zechmann@med.uni-heidelberg.de

M. Eder · M. Eisenhut
Department of Radiopharmaceutical Chemistry, German Cancer Research Center, Im Neuenheimer Feld 280,
Heidelberg, Germany

M. Eder
e-mail: m.eder@dkfz.de

M. Eisenhut
e-mail: m.eisenhut@dkfz.de

H. G. Linhart
National Center for Tumor Diseases (NCT)/DKFZ,
Im Neuenheimer Feld 581,
69120 Heidelberg, Germany
e-mail: heinz.linhart@med.uni-heidelberg.de

B. A. Hadaschik
Department of Urology, University Hospital of Heidelberg,
Im Neuenheimer Feld 110,
Heidelberg, Germany
e-mail: boris.hadaschik@med.uni-heidelberg.de

T. Holland-Letz
Department of Biostatistics, German Cancer Research Center,
Im Neuenheimer Feld 280,
Heidelberg, Germany
e-mail: t.holland-letz@dkfz.de

U. Haberkorn
Clinical Cooperation Unit Nuclear Medicine, German Cancer Research Centre, Heidelberg, Germany

PET imaging with a [^{68}Ga]gallium-labelled PSMA ligand for the diagnosis of prostate cancer: biodistribution in humans and first evaluation of tumour lesions

A. Afshar-Oromieh , A. Malcher , M. Eder , M. Eisenhut , H. G. Linhart , B. A. Hadaschik , T. Holland-Letz , F. L. Giesel , C. Kratochwil et al.

Methods

A total of 37 patients with PC and rising prostate-specific antigen (PSA) levels were subjected to ^{68}Ga-PSMA positron emission tomography (PET)/CT. Quantitative assessment of tracer uptake was performed 1 and 3 h post-injection (p.i.) by analysis of mean and maximum standardized uptake values ($SUV_{mean/max}$) of several organs and 65 tumour lesions. Subsequently, tumour to background ratios were calculated.

Results

The PET/CT images showed intense tracer uptake in both kidneys and salivary glands. Moderate uptake was seen in lacrimal glands, liver, spleen and in small and large bowel. Quantitative assessment revealed excellent contrast between tumour lesions and most normal tissues. Of 37 patients, 31 (83.8 %) showed at least one lesion suspicious for cancer at a detection rate of 60 % at PSA <2.2 ng/ml and 100 % at PSA >2.2 ng/ml. Median tumour to background ratios were 18.8 (2.4–158.3) in early images and 28.3 (2.9–224.0) in late images.

Conclusion

The biodistribution of the novel ^{68}Ga-PSMA tracer and its ability to detect PC lesions was analysed in 37 patients. Within healthy organs, kidneys and salivary glands demonstrated the highest radiotracer uptake. Lesions suspicious for PC presented with excellent contrast as early as 1 h p.i. with high detection rates even at low PSA levels.

Biodistribuzione

Colina

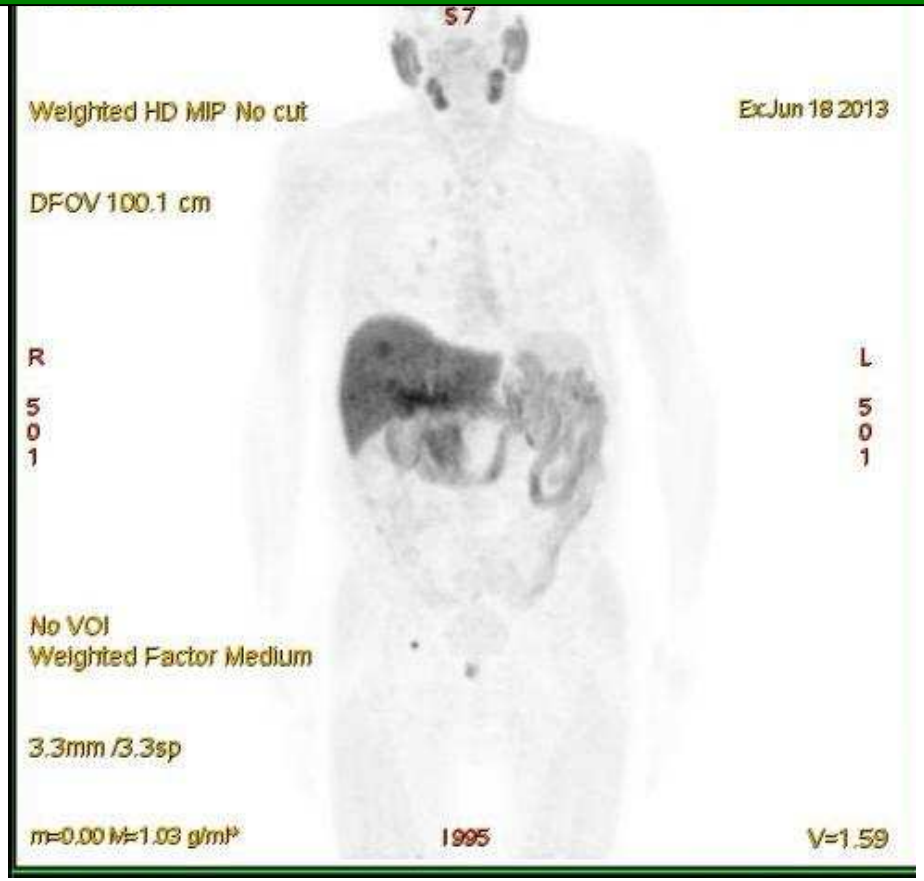

PSMA

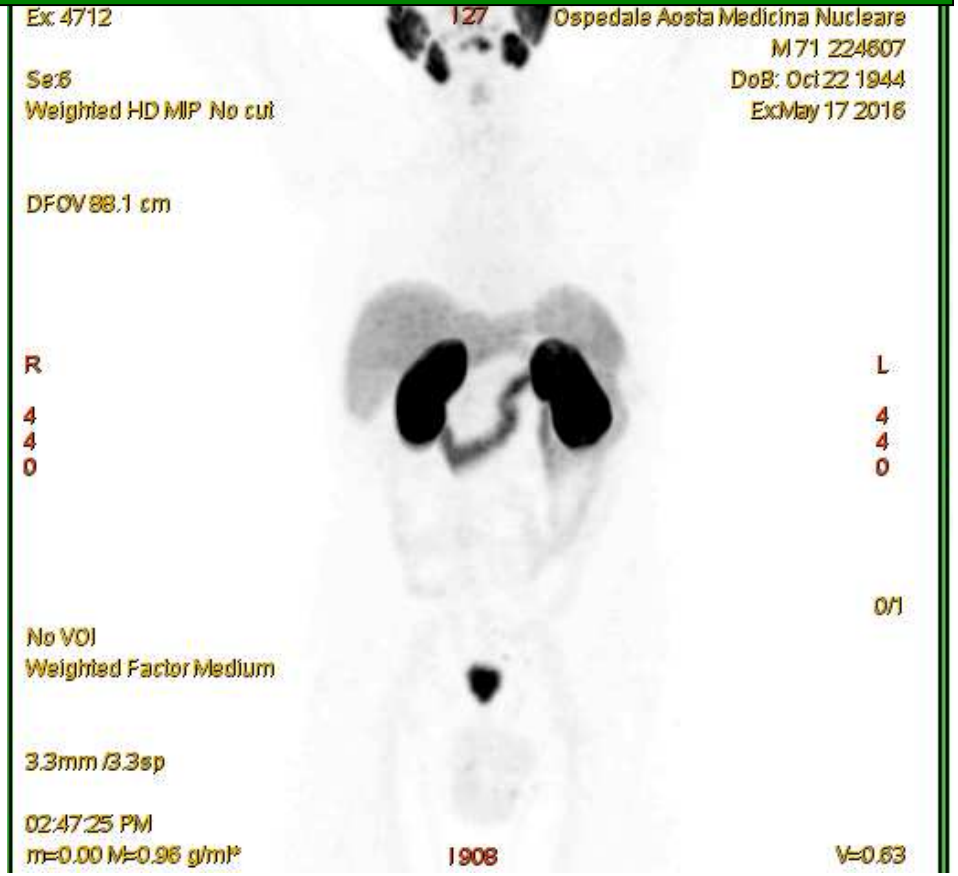

Eur J Nucl Med Mol Imaging (2015) 42:197–209
DOI 10.1007/s00259-014-2949-6

ORIGINAL ARTICLE

The diagnostic value of PET/CT imaging with the ^{68}Ga-labelled PSMA ligand HBED-CC in the diagnosis of recurrent prostate cancer

Ali Afshar-Oromieh · Eleni Avtzi · Frederik L. Giesel · Tim Holland-Letz · Heinz G. Linhart · Matthias Eder · Michael Eisenhut · Silvan Boxler · Boris A. Hadaschik · Clemens Kratochwil · Wilko Weichert · Klaus Kopka · Jürgen Debus · Uwe Haberkorn

Received: 5 June 2014 / Accepted: 8 October 2014 / Published online: 20 November 2014

Abstract
Purpose Since the introduction of positron emission tomography (PET) imaging with ^{68}Ga-PSMA-HBED-CC (= ^{68}Ga-DKFZ-PSMA-11), this method has been regarded as a significant step forward in the diagnosis of recurrent prostate cancer (PCa). However, published data exist for small patient cohorts only. The aim of this evaluation was to analyse the diagnostic value of ^{68}Ga-PSMA-ligand PET/CT in a large cohort and the influence of several possibly interacting variables.
Methods We performed a retrospective analysis in 319 patients who underwent ^{68}Ga-PSMA-ligand PET/CT from 2011 to 2014. Potential influences of several factors such as prostate-specific antigen (PSA) level and doubling time (DT), Gleason score (GSC), androgen deprivation therapy

Electronic supplementary material The online version of this article (doi:10.1007/s00259-014-2949-6) contains supplementary material, which is available to authorized users.

A. Afshar-Oromieh (✉) · E. Avtzi · F. L. Giesel · C. Kratochwil · U. Haberkorn
Department of Nuclear Medicine, University Hospital of Heidelberg, Im Neuenheimer Feld 400, 69120 Heidelberg, Germany
e-mail: a.afshar@gmx.de

E. Avtzi
e-mail: thessalonikia90@web.de

F. L. Giesel
e-mail: f.giesel@dkfz.de

C. Kratochwil
e-mail: clemens.kratochwil@med.uni-heidelberg.de

U. Haberkorn
e-mail: uwe.haberkorn@med.uni-heidelberg.de

A. Afshar-Oromieh · F. L. Giesel · C. Kratochwil · U. Haberkorn
German Cancer Research Centre, Clinical Cooperation Unit Nuclear Medicine, Heidelberg, Germany

T. Holland-Letz
Department of Biostatistics, German Cancer Research Center, Im Neuenheimer Feld 280, Heidelberg, Germany
e-mail: t.holland-letz@dkfz.de

H. G. Linhart
National Centre for Tumor Diseases (NCT), German Cancer Research Centre, Heidelberg, Im Neuenheimer Feld 581, 69120 Heidelberg, Germany
e-mail: heinz.linhart@med.uni-heidelberg.de

M. Eder · M. Eisenhut · K. Kopka
Division of Radiopharmaceutical Chemistry, German Cancer Research Center, Im Neuenheimer Feld 280, Heidelberg, Germany

M. Eder
e-mail: m.eder@dkfz.de

M. Eisenhut
e-mail: m.eisenhut@kabelbw.de

K. Kopka
e-mail: k.kopka@dkfz.de

S. Boxler · B. A. Hadaschik
Department of Urology, University Hospital of Heidelberg, Im Neuenheimer Feld 110, Heidelberg, Germany

S. Boxler
e-mail: silvanboxler@gmx.ch

B. A. Hadaschik
e-mail: boris.hadaschik@med.uni-heidelberg.de

W. Weichert
Department of Pathology, University Hospital of Heidelberg, Im Neuenheimer Feld 224, 69120 Heidelberg, Germany
e-mail: wilko.weichert@med.uni-heidelberg.de

J. Debus
Department of Radiation Oncology and Therapy, University Hospital Heidelberg, Im Neuenheimer Feld 400, 69120 Heidelberg, Germany
e-mail: Juergen.Debus@med.uni-heidelberg.de

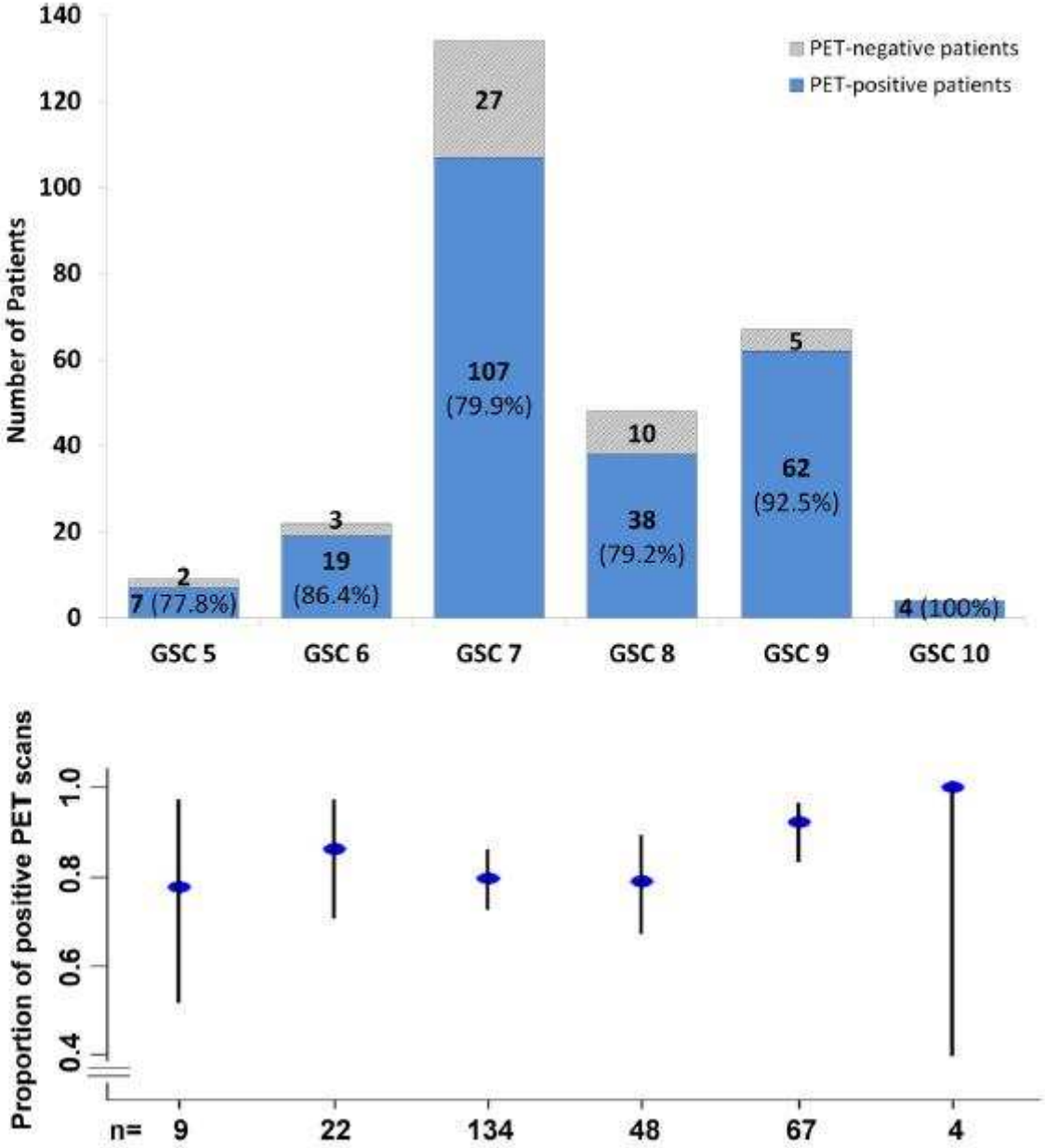

Fig. 4 Probability of a pathological ^{68}Ga-PSMA-ligand PET/CT as histogram (*above*) and plot of the rates of pathological PET/CTs with confidence intervals (*below*) depending on GSC in 284 patients. *Blue columns* include the number of pathological PET/CTs and their rate in %

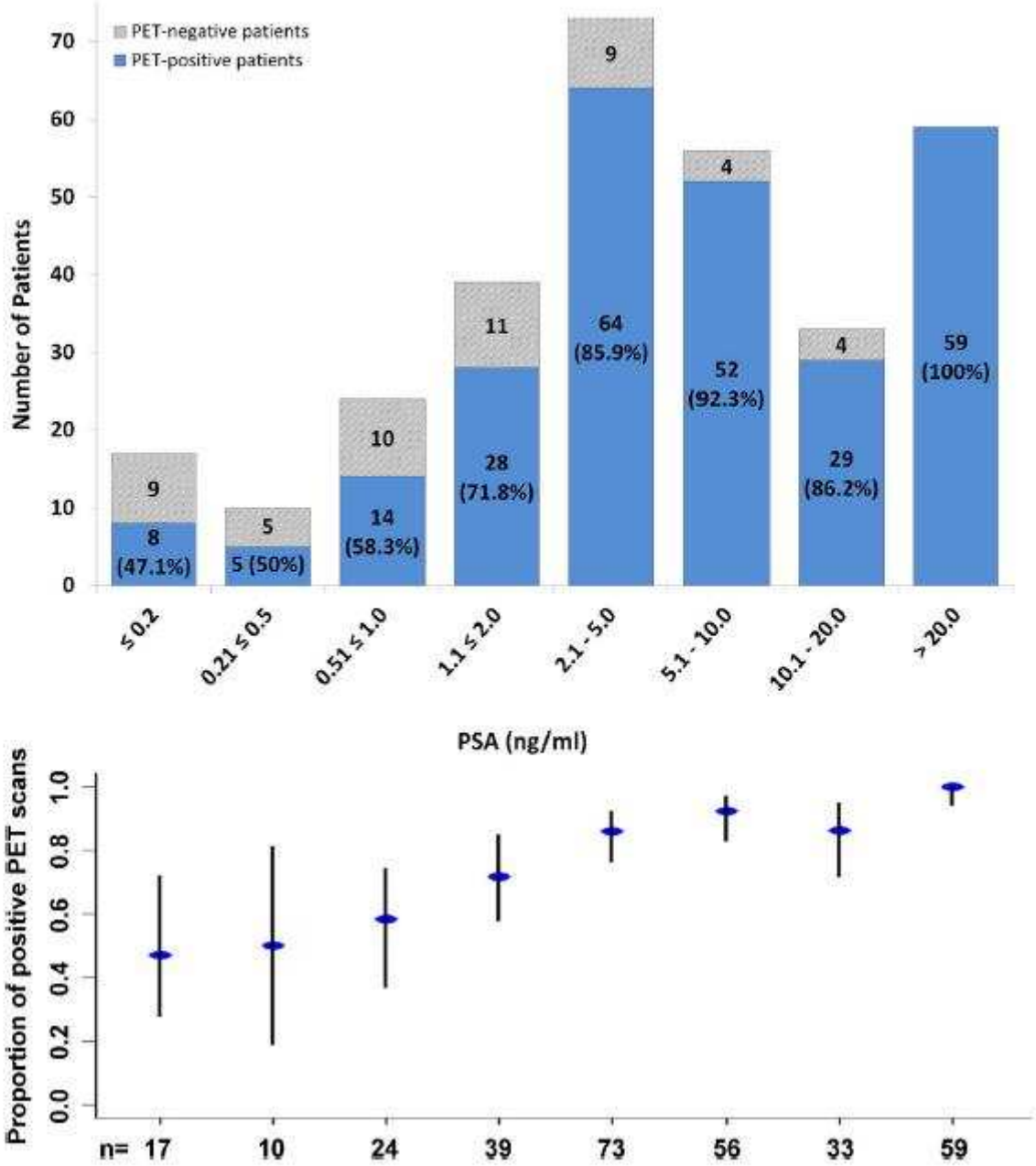

Fig. 3 Probability of a pathological ^{68}Ga-PSMA-ligand PET/CT as histogram (*above*) and plot of the rates of pathological PET/CTs with confidence intervals (*below*) depending on PSA levels in 311 patients. *Blue columns* include the number of pathological PET/CTs and their rate in %

Evaluation of Hybrid ^{68}Ga-PSMA Ligand PET/CT in 248 Patients with Biochemical Recurrence After Radical Prostatectomy

Matthias Eiber*[1,2], Tobias Maurer*[3], Michael Souvatzoglou[1], Ambros J. Beer[1,4], Alexander Ruffani[1], Bernhard Haller[5], Frank-Philipp Graner[1], Hubert Kübler[3], Uwe Haberhorn[6], Michael Eisenhut[6], Hans-Jürgen Wester[7], Jürgen E. Gschwend[3], and Markus Schwaiger[1]

[1]Department of Nuclear Medicine, Klinikum Rechts der Isar, Technische Universität München, Munich, Germany; [2]Department of Radiology, Klinikum Rechts der Isar, Technische Universität München, Munich, Germany; [3]Department of Urology, Klinikum Rechts der Isar, Technische Universität München, Munich, Germany; [4]Department of Nuclear Medicine, University Hospital Ulm, Ulm, Germany; [5]Klinikum Rechts der Isar, Institute of Medical Statistics and Epidemiology, Technische Universität München, Munich, Germany; [6]Department of Nuclear Medicine, University Hospital of Heidelberg, Heidelberg, Germany; and [7]Technische Universität München, Pharmaceutical Radiochemistry, Garching, Germany

The expression of prostate-specific membrane antigen (PSMA) is increased in prostate cancer. Recently, ^{68}Ga-PSMA (Glu-NH-CO-NH-Lys-(Ahx)-[^{68}Ga(HBED-CC)]) was developed as a PSMA ligand. The aim of this study was to investigate the detection rate of ^{68}Ga-PSMA PET/CT in patients with biochemical recurrence after radical

Key Words: PSMA ligand; PET/CT; hybrid imaging; prostate cancer; biochemical recurrence

J Nucl Med 2015; 56:668–674
DOI: 10.2967/jnumed.115.154153

Evaluation of Hybrid ^{68}Ga-PSMA Ligand PET/CT in 248 Patients with Biochemical Recurrence After Radical Prostatectomy

Matthias Eiber*[1,2], Tobias Maurer*[3], Michael Souvatzoglou[1], Ambros J. Beer[1,4], Alexander Ruffani[1], Bernhard Haller[5], Frank-Philipp Graner[1], Hubert Kübler[3], Uwe Haberhorn[6], Michael Eisenhut[6], Hans-Jürgen Wester[7], Jürgen E. Gschwend[3], and Markus Schwaiger[1]

[1]Department of Nuclear Medicine, Klinikum Rechts der Isar, Technische Universität München, Munich, Germany; [2]Department of Radiology, Klinikum Rechts der Isar, Technische Universität München, Munich, Germany; [3]Department of Urology, Klinikum Rechts der Isar, Technische Universität München, Munich, Germany; [4]Department of Nuclear Medicine, University Hospital Ulm, Ulm, Germany; [5]Klinikum Rechts der Isar, Institute of Medical Statistics and Epidemiology, Technische Universität München, Munich, Germany; [6]Department of Nuclear Medicine, University Hospital of Heidelberg, Heidelberg, Germany; and [7]Technische Universität München, Pharmaceutical Radiochemistry, Garching, Germany

The expression of prostate-specific membrane antigen (PSMA) is increased in prostate cancer. Recently, ^{68}Ga-PSMA (Glu-NH-CO-NH-Lys-(Ahx)-[^{68}Ga(HBED-CC)]) was developed as a PSMA ligand. The aim of this study was to investigate the detection rate of ^{68}Ga-PSMA PET/CT in patients with biochemical recurrence after radical prostatectomy. **Methods:** Two hundred forty-eight of 393 patients were evaluable for a retrospective analysis. Median prostate-specific antigen (PSA) level was 1.99 ng/mL (range, 0.2–59.4 ng/mL). All patients underwent contrast-enhanced PET/CT after injection of 155 ± 27 MBq of ^{68}Ga-PSMA ligand. The detection rates were correlated with PSA level and PSA kinetics. The influence of antihormonal treatment, primary Gleason score, and contribution of PET and morphologic imaging to the final diagnosis were assessed. **Results:** Two hundred twenty-two (89.5%) patients showed pathologic findings in ^{68}Ga-PSMA ligand PET/CT. The detection rates were 96.8%, 93.0%, 72.7%, and 57.9% for PSA levels of ≥2, 1 to <2, 0.5 to <1, and 0.2 to <0.5 ng/mL, respectively. Whereas detection rates increased with a higher PSA velocity (81.8%, 82.4%, 92.1%, and 100% in <1, 1 to <2, 2 to <5, and ≥5 ng/mL/y, respectively), no significant association could be found for PSA doubling time (82.7%, 96.2%, and 90.7% in >6, 4–6, and <4 mo, respectively). ^{68}Ga-PSMA ligand PET (as compared with CT) exclusively provided pathologic findings in 81 (32.7%) patients. In 61 (24.6%) patients, it exclusively identified additional involved regions. In higher Gleason score (≤7 vs. ≥8), detection efficacy was significantly increased (P = 0.0190). No significant difference in detection efficacy was present regarding antiandrogen therapy (P = 0.0783). **Conclusion:** Hybrid ^{68}Ga-PSMA ligand PET/CT shows substantially higher detection rates than reported for other imaging modalities. Most importantly, it reveals a high number of positive findings in the clinically important range of low PSA values (<0.5 ng/mL), which in many cases can substantially influence the further clinical management.

Received Jan. 9, 2015; revision accepted Mar. 5, 2015.
For correspondence or reprints contact: Matthias Eiber, Department of Nuclear Medicine, Ismaninger Strasse 22, 81675 Munich, Germany.
E-mail: matthias.eiber@tum.de
*Contributed equally to this work.
Published online Mar. 19, 2015.

Key Words: PSMA ligand; PET/CT; hybrid imaging; prostate cancer; biochemical recurrence

J Nucl Med 2015; 56:668–674
DOI: 10.2967/jnumed.115.154153

In biochemical recurrence after radical prostatectomy (RP), an increase of the prostate-specific antigen (PSA) level precedes a clinically detectable recurrence by months to years (*1*). However, it cannot differentiate between local, regional, or systemic disease with the necessary precision that is essential for further disease management (*2*). Furthermore, PSA kinetics such as PSA velocity (PSAvel) and PSA doubling time (PSAdt) play an important role, with high PSA kinetics facilitating disease detection (*3*).

Morphologic imaging methods exhibit considerable limitations: sensitivity ranges between 25% and 54% for the detection of local recurrence by transrectal ultrasound or CT and is moderately improved using functional MR imaging techniques (*2,4*). The sensitivity for detection of lymph node metastases of CT or MR imaging is reported to be 30%–80% (*5*). Ultra-small particles of iron oxides proved to be effective; however, they have not been approved by regulatory authorities so far (*6*).

Various targets have been addressed by molecular imaging to improve the detection of recurrent prostate cancer (PC). For PET imaging, mainly ^{11}C- and ^{11}F-labeled choline derivates have been used in the past (*7–9*). However, especially in patients with PSA values below 3 ng/mL, the detection rate is only 40%–60% (*3,4,7*). Recently, a new molecular probe targeting, for example, the gastrin-releasing peptide receptor or the prostate-specific membrane antigen (PSMA), has been developed (*10–12*). PSMA is a membrane-bound enzyme with significantly elevated expression in PC cells in comparison to benign prostatic tissue (*13*). The localization of the catalytic site of PSMA in the extracellular domain allows the development of small specific inhibitors that are internalized after ligand binding (*14*). Older agents targeting the intracellular domain of PSMA showed disappointing results due to low image contrast, low sensitivity, or high background signal (*15*). The recent development

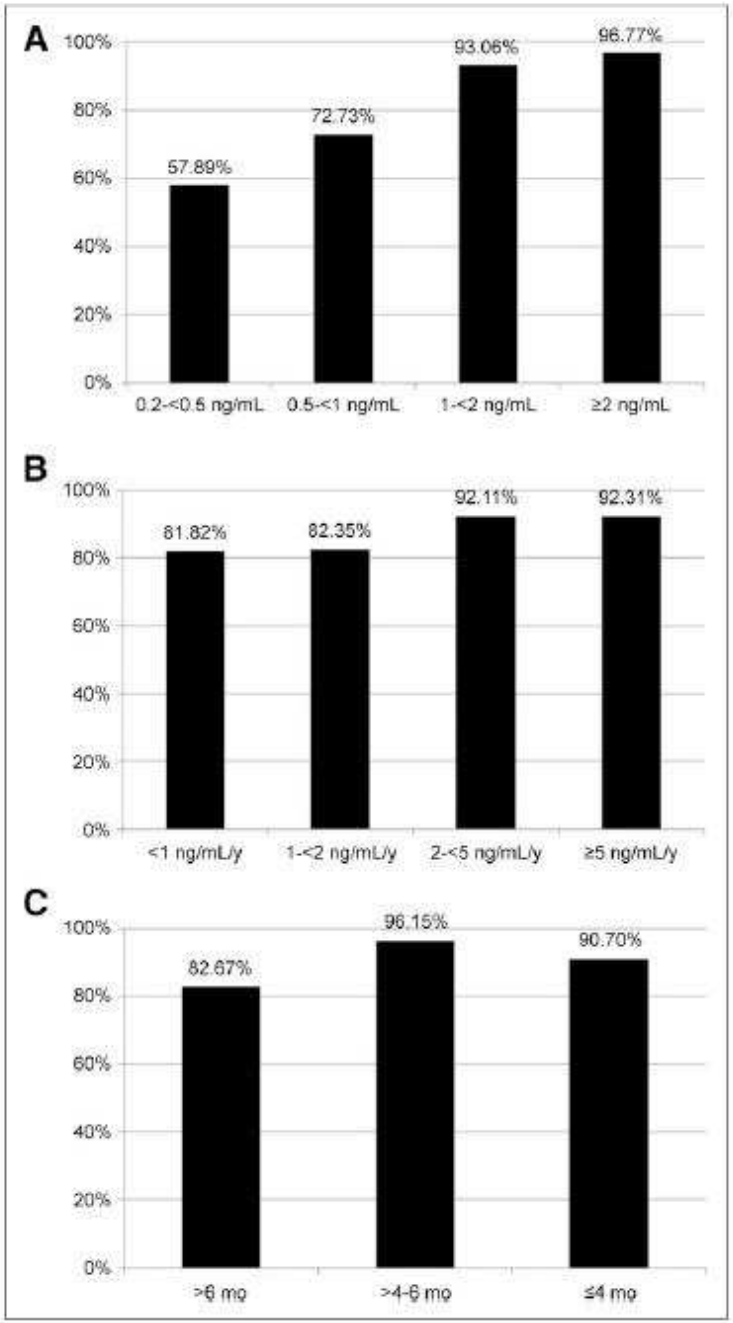

FIGURE 2. Detection rate of ^{68}Ga-PSMA ligand PET/CT in relation PSA level (A), PSAvel (B), and PSAdt (C).

PSMA

ABX advanced biochemical compounds

Catalogue Number	Product	Order number / Unit
9920	**PSMA-11**	9920.0003.5: 0.5 mg per vial 9920.0001: 1 mg per vial Please inquire for customized filling and bulk quantities.

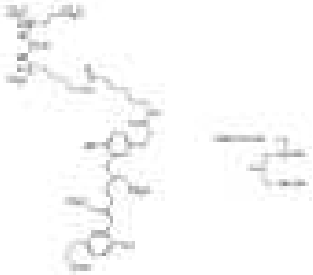

Precursor for [^{68}Ga]GaPSMA-11
PSMA: prostate-specific membrane antigen

Molar Mass: 947.0 (net peptide)

$C_{44}H_{62}N_6O_{17} \cdot x\,CF_3CO_2H$

[1366302-52-4]

Colourless to off-white solid packaged in dark glass screw cap vials.

Purity: ≥ 95 %

Certificates:
CoA; MS (identity); HPLC (purity)

Chemical Name:
CA Index name: 4,6,12,19-Tetraazadocosane-1,3,7-tricarboxylic acid, 22-[3-[[[2-[[[5-(2-carboxyethyl)-2-hydroxyphenyl]methyl](carboxymethyl)amino]ethyl](carboxymethyl)amino]methyl]-4-hydroxyphenyl]-5,13,20-trioxo-, (3S,7S)-, supplied as trifluoroacetate salt

Synonymes:
PSMA$^{11[68]}$; Glu-CO-Lys(Ahx)-HBED-CC; Glu-NH-CO-NH-Lys(Ahx)-HBED-CC; 2-[3-(1-Carboxy-5-{6-[3-(3-{[2-[[5-(2-carboxy-ethyl)-2-hydroxy-benzyl]-carboxymethyl-amino]-ethyl}-carboxymethyl-amino)-methyl]-4-hydroxy-phenyl}-propionylamino)-hexanoylamino]-

Literature:

Eder M. et al. Novel Preclinical and Radiopharmaceutical Aspects of [^{68}Ga]Ga-PSMA-HBED-CC: A New PET Tracer for Imaging of Prostate Cancer. Pharmaceuticals. 2014, 7, 779-796.

Eder M. et al. ^{68}Ga-Complex Lipophilicity and the Targeting Property of a Urea-Based PSMA Inhibitor for PET Imaging. Bioconjugate Chem. 2012, 23, 688-697.

date of product catalogue issue: 30 July 2015

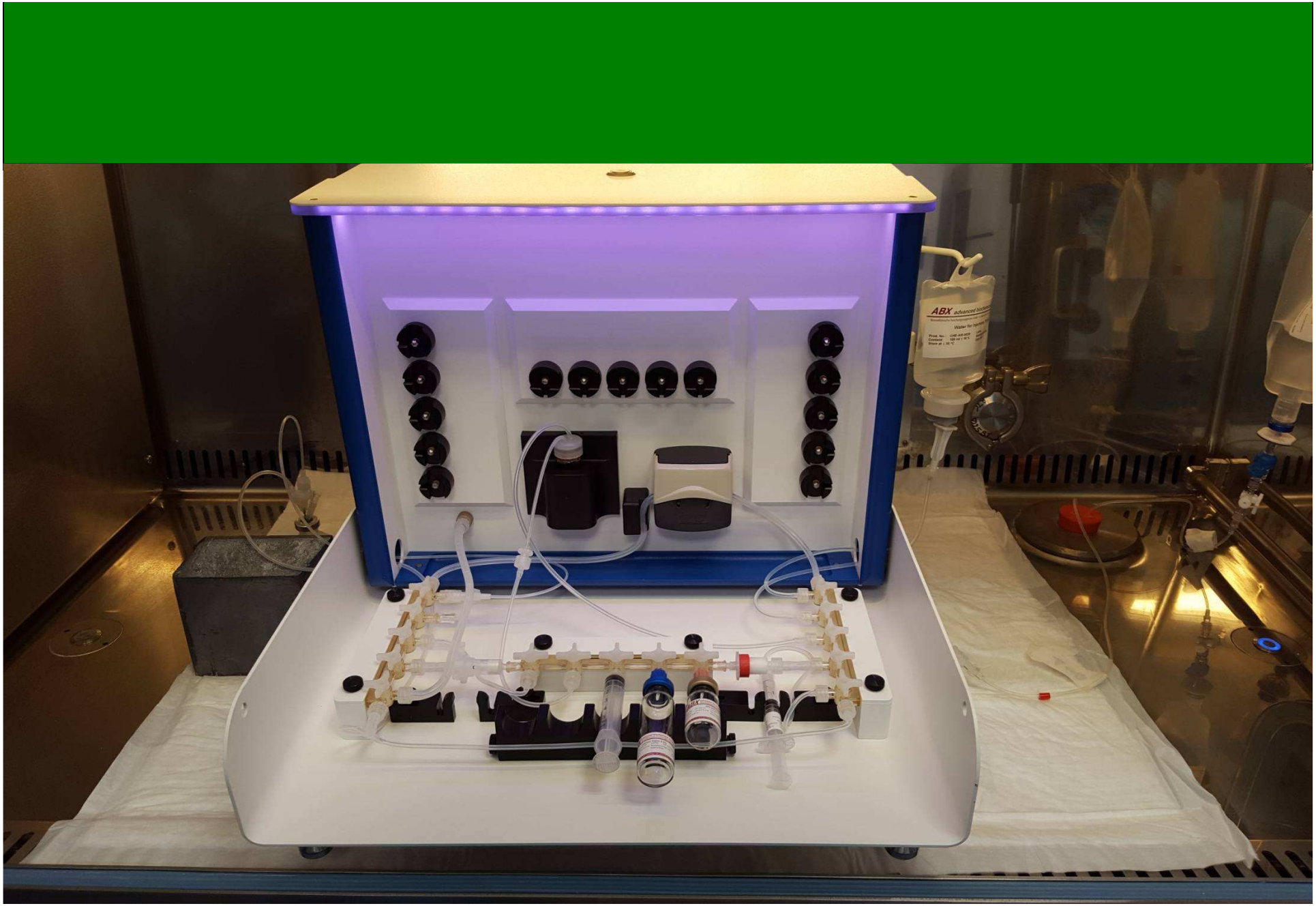
ABX

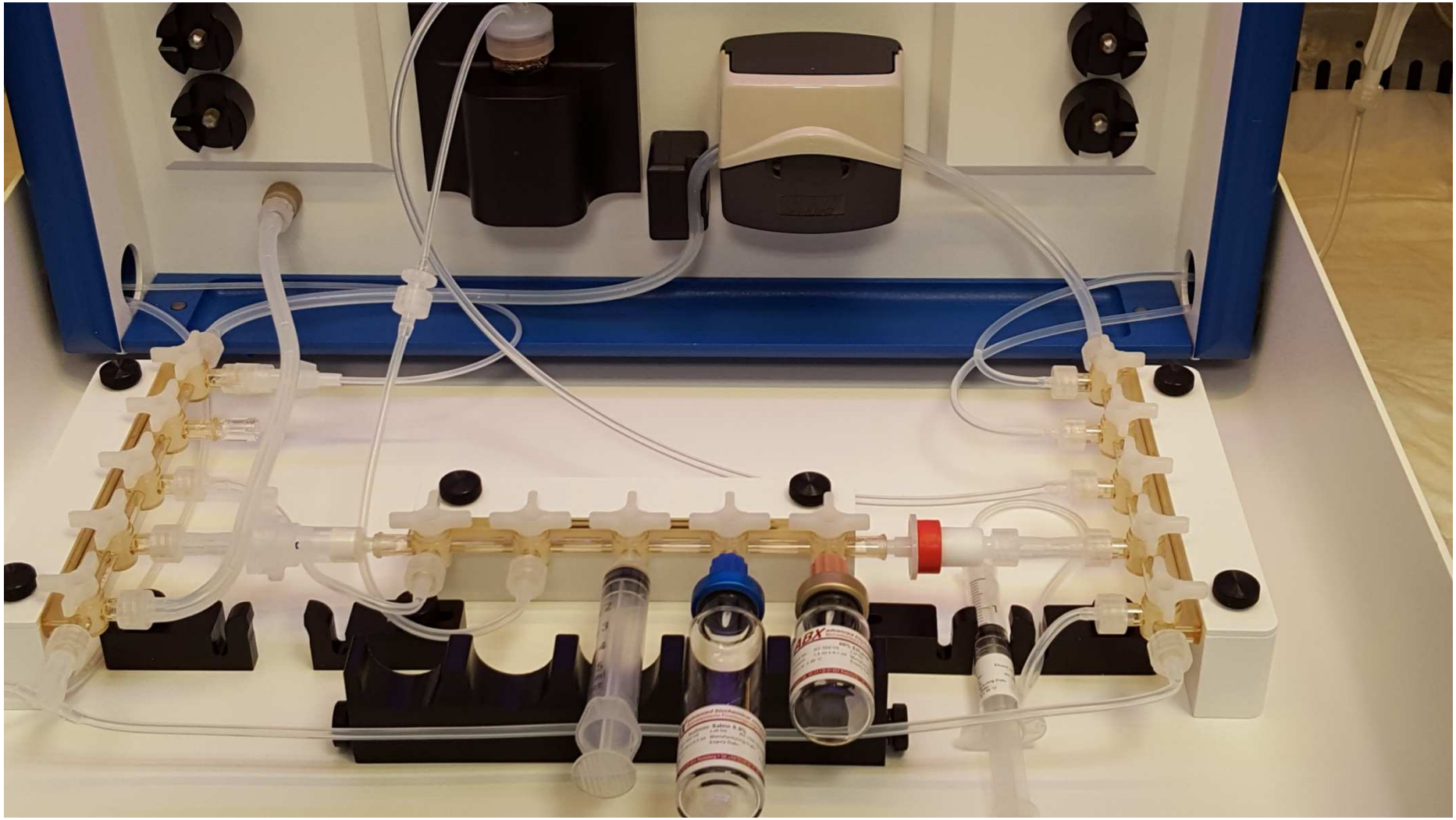

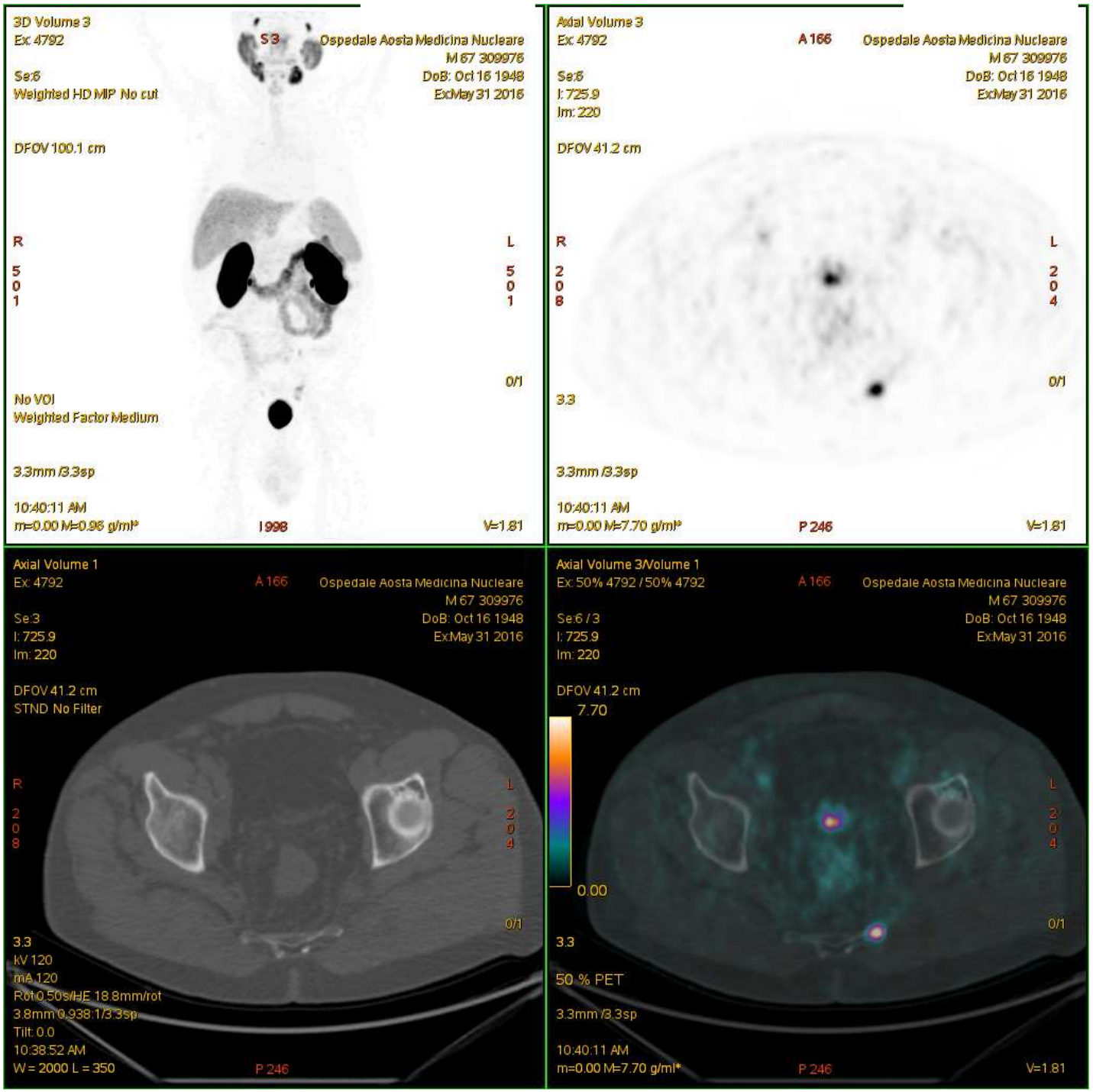
3D Volume 3
Ex: 4792
S 3
Ospedale Aosta Medicina Nucleare
M 67 309976
Se:6
DoB: Oct 16 1948
Weighted HD MIP No cut
Ex:May 31 2016
DFOV 100.1 cm
R
L
5
0
1
5
0
1
0/1
No VOI
Weighted Factor Medium
3.3mm /3.3sp
10:40:11 AM
m=0.00 M=0.96 g/ml*
I 998
V=1.81
Axial Volume 3
Ex: 4792
A 166
Ospedale Aosta Medicina Nucleare
M 67 309976
Se:6
DoB: Oct 16 1948
I: 725.9
Ex:May 31 2016
Im: 220
DFOV 41.2 cm
R
L
2
0
8
2
0
4
0/1
3.3
3.3mm /3.3sp
10:40:11 AM
m=0.00 M=7.70 g/ml*
P 246
V=1.81
Axial Volume 1
Ex: 4792
A 166
Ospedale Aosta Medicina Nucleare
M 67 309976
Se:3
DoB: Oct 16 1948
I: 725.9
Ex:May 31 2016
Im: 220
DFOV 41.2 cm
STND No Filter
R
L
2
0
8
2
0
4
0/1
3.3
kV 120
mA 120
Rot 0.50s/HE 18.8mm/rot
3.8mm 0.938:1/3.3sp
Tilt: 0.0
10:38:52 AM
W = 2000 L = 350
P 246
Axial Volume 3/Volume 1
Ex: 50% 4792 / 50% 4792
A 166
Ospedale Aosta Medicina Nucleare
M 67 309976
Se:6 / 3
DoB: Oct 16 1948
I: 725.9
Ex:May 31 2016
Im: 220
DFOV 41.2 cm
7.70
0.00
R
L
2
0
8
2
0
4
0/1
3.3
50 % PET
3.3mm /3.3sp
10:40:11 AM
m=0.00 M=7.70 g/ml*
P 246
V=1.81

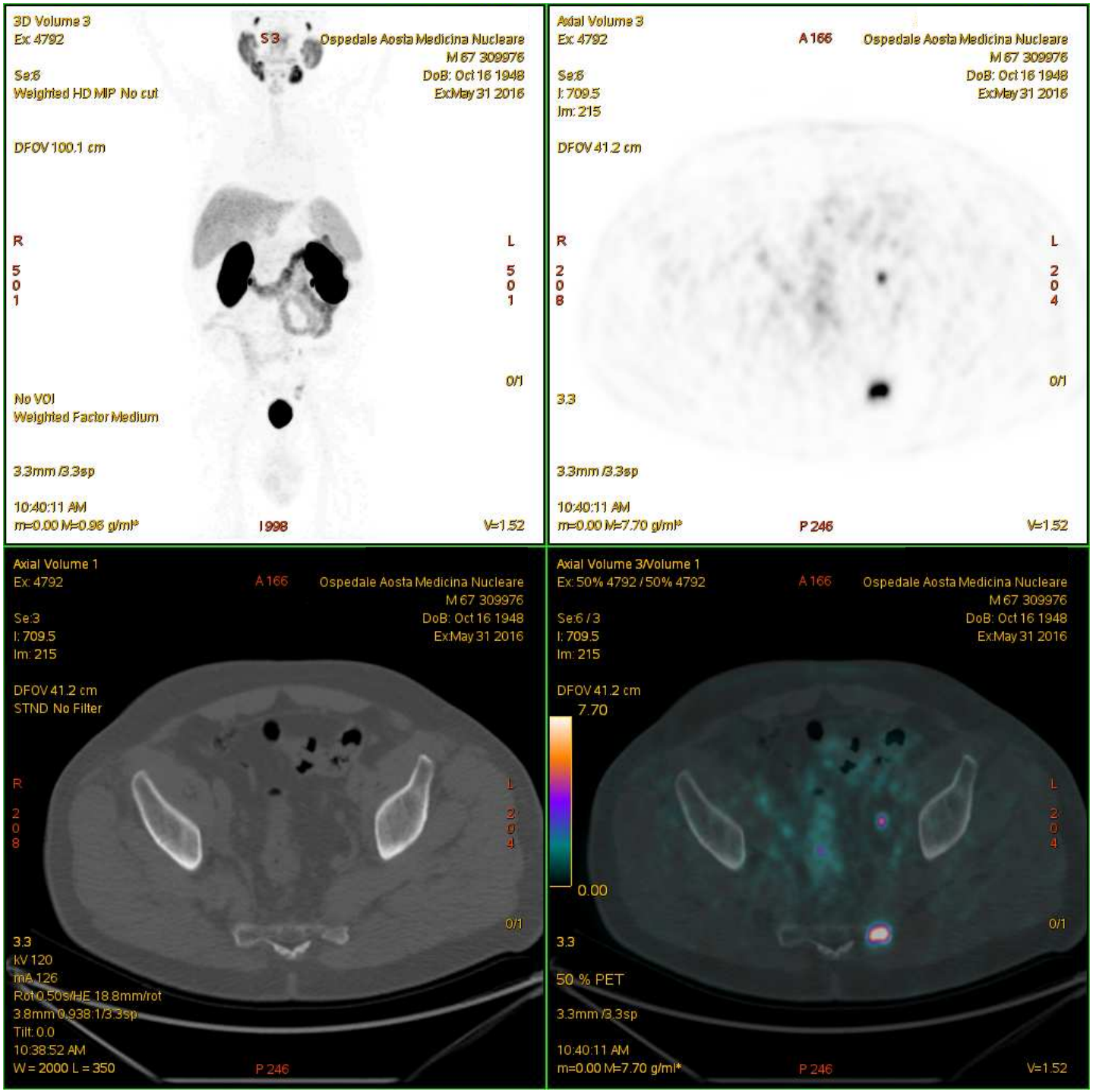
3D Volume 3
Ex: 4792
S 3
Ospedale Aosta Medicina Nucleare
M 67 309976
DoB: Oct 16 1948
Ex:May 31 2016
Se:6
Weighted HD MIP No cut
DFOV 100.1 cm
R
L
5 0 1
5 0 1
0/1
No VOI
Weighted Factor Medium
3.3mm /3.3sp
10:40:11 AM
m=0.00 M=0.96 g/ml*
I 998
V=1.52
Axial Volume 3
Ex: 4792
A 166
Ospedale Aosta Medicina Nucleare
M 67 309976
DoB: Oct 16 1948
Ex:May 31 2016
Se:6
I: 709.5
Im: 215
DFOV 41.2 cm
R
L
2 0 8
2 0 4
0/1
3.3
3.3mm /3.3sp
10:40:11 AM
m=0.00 M=7.70 g/ml*
P 246
V=1.52
Axial Volume 1
Ex: 4792
A 166
Ospedale Aosta Medicina Nucleare
M 67 309976
DoB: Oct 16 1948
Ex:May 31 2016
Se:3
I: 709.5
Im: 215
DFOV 41.2 cm
STND No Filter
R
L
2 0 8
2 0 4
0/1
3.3
kV 120
mA 126
Rot 0.50s/HE 18.8mm/rot
3.8mm 0.938:1/3.3sp
Tilt: 0.0
10:38:52 AM
W = 2000 L = 350
P 246
Axial Volume 3/Volume 1
Ex: 50% 4792 / 50% 4792
A 166
Ospedale Aosta Medicina Nucleare
M 67 309976
DoB: Oct 16 1948
Ex:May 31 2016
Se:6 / 3
I: 709.5
Im: 215
DFOV 41.2 cm
7.70
0.00
R
L
2 0 8
2 0 4
0/1
3.3
50 % PET
3.3mm /3.3sp
10:40:11 AM
m=0.00 M=7.70 g/ml*
P 246
V=1.52

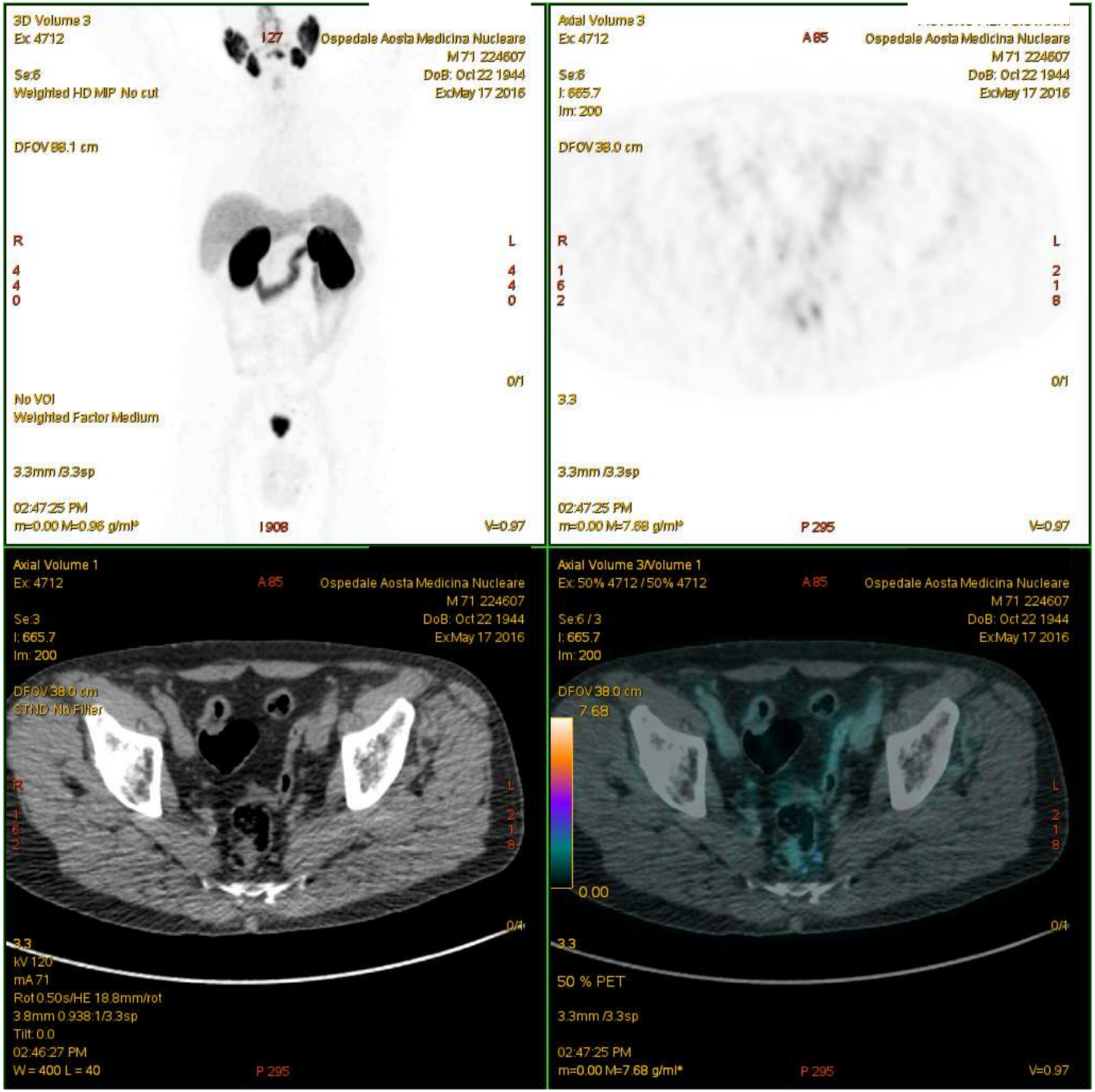
3D Volume 3
Ex: 4712
I27
Ospedale Aosta Medicina Nucleare
M 71 224607
DoB: Oct 22 1944
Ex:May 17 2016
Se:6
Weighted HD MIP No cut
DFOV 88.1 cm
R
L
No VOI
Weighted Factor Medium
3.3mm /3.3sp
02:47:25 PM
m=0.00 M=0.96 g/ml*
I 908
V=0.97
Axial Volume 3
Ex: 4712
A 85
Ospedale Aosta Medicina Nucleare
M 71 224607
DoB: Oct 22 1944
Ex:May 17 2016
Se:6
I: 665.7
Im: 200
DFOV 38.0 cm
R
L
3.3
3.3mm /3.3sp
02:47:25 PM
m=0.00 M=7.68 g/ml*
P 295
V=0.97
Axial Volume 1
Ex: 4712
A 85
Ospedale Aosta Medicina Nucleare
M 71 224607
DoB: Oct 22 1944
Ex:May 17 2016
Se:3
I: 665.7
Im: 200
DFOV 38.0 cm
STND No Filter
R
L
3.3
kV 120
mA 71
Rot 0.50s/HE 18.8mm/rot
3.8mm 0.938:1/3.3sp
Tilt: 0.0
02:46:27 PM
W = 400 L = 40
P 295
Axial Volume 3/Volume 1
Ex: 50% 4712 / 50% 4712
A 85
Ospedale Aosta Medicina Nucleare
M 71 224607
DoB: Oct 22 1944
Ex:May 17 2016
Se:6 / 3
I: 665.7
Im: 200
DFOV 38.0 cm
7.68
0.00
R
L
3.3
50 % PET
3.3mm /3.3sp
02:47:25 PM
m=0.00 M=7.68 g/ml*
P 295
V=0.97

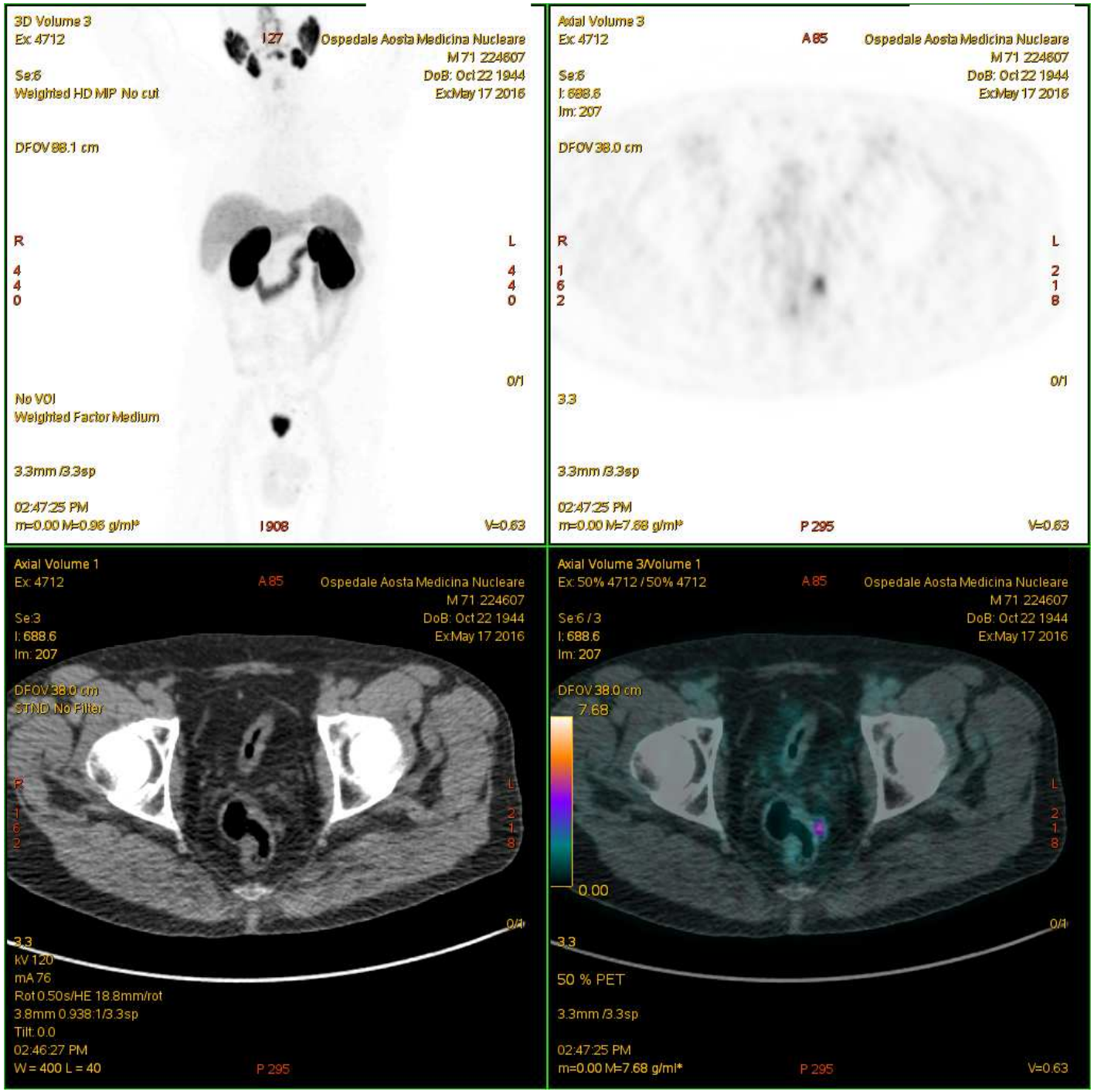
3D Volume 3
Ex: 4712
I 27
Ospedale Aosta Medicina Nucleare
M 71 224607
Se:6
DoB: Oct 22 1944
Weighted HD MIP No cut
Ex:May 17 2016
DFOV 88.1 cm
R
L
4
4
0
4
4
0
0/1
No VOI
Weighted Factor Medium
3.3mm /3.3sp
02:47:25 PM
m=0.00 M=0.96 g/ml*
I 908
V=0.63
Axial Volume 3
Ex: 4712
A 85
Ospedale Aosta Medicina Nucleare
M 71 224607
Se:6
DoB: Oct 22 1944
I: 688.6
Ex:May 17 2016
Im: 207
DFOV 38.0 cm
R
L
1
6
2
2
1
8
0/1
3.3
3.3mm /3.3sp
02:47:25 PM
m=0.00 M=7.68 g/ml*
P 295
V=0.63
Axial Volume 1
Ex: 4712
A 85
Ospedale Aosta Medicina Nucleare
M 71 224607
Se:3
DoB: Oct 22 1944
I: 688.6
Ex:May 17 2016
Im: 207
DFOV 38.0 cm
STND No Filter
R
L
1
6
2
2
1
8
0/1
3.3
kV 120
mA 76
Rot 0.50s/HE 18.8mm/rot
3.8mm 0.938:1/3.3sp
Tilt: 0.0
02:46:27 PM
W = 400 L = 40
P 295
Axial Volume 3/Volume 1
Ex: 50% 4712 / 50% 4712
A 85
Ospedale Aosta Medicina Nucleare
M 71 224607
Se:6 / 3
DoB: Oct 22 1944
I: 688.6
Ex:May 17 2016
Im: 207
DFOV 38.0 cm
7.68
0.00
L
2
1
8
0/1
3.3
50 % PET
3.3mm /3.3sp
02:47:25 PM
m=0.00 M=7.68 g/ml*
P 295
V=0.63

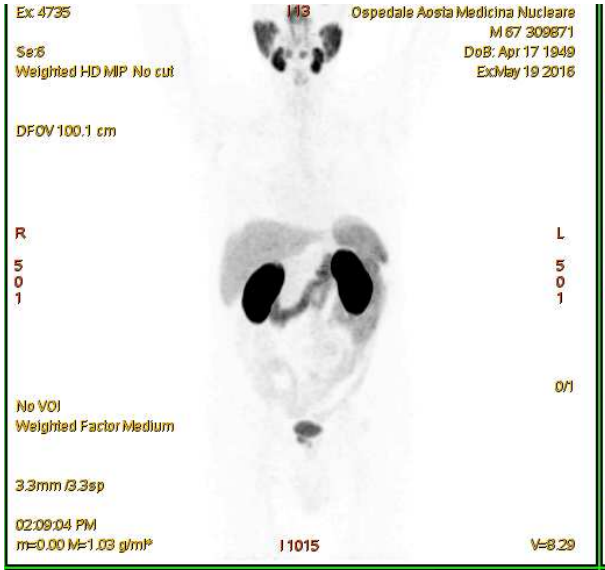
Ex: 4735
I 13
Ospedale Aosta Medicina Nucleare
M 67 309871
Se:6
DoB: Apr 17 1949
Weighted HD MIP No cut
ExMay 19 2016
DFOV 100.1 cm
R
L
5
0
1
5
0
1
0/1
No VOI
Weighted Factor Medium
3.3mm /3.3sp
02:09:04 PM
m=0.00 M=1.03 g/ml*
I 1015
V=8.29

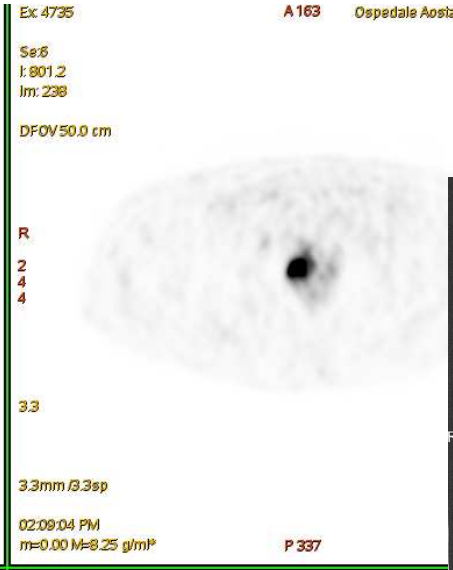
Ex: 4735
A 163
Ospedale Aosta Medicina Nucleare
M 67 309871
Se:6
DoB: Apr 17 1949
I: 801.2
ExMay 19 2016
Im: 238
DFOV 50.0 cm
R
2
4
4
3.3
3.3mm /3.3sp
02:09:04 PM
m=0.00 M=8.25 g/ml*
P 337

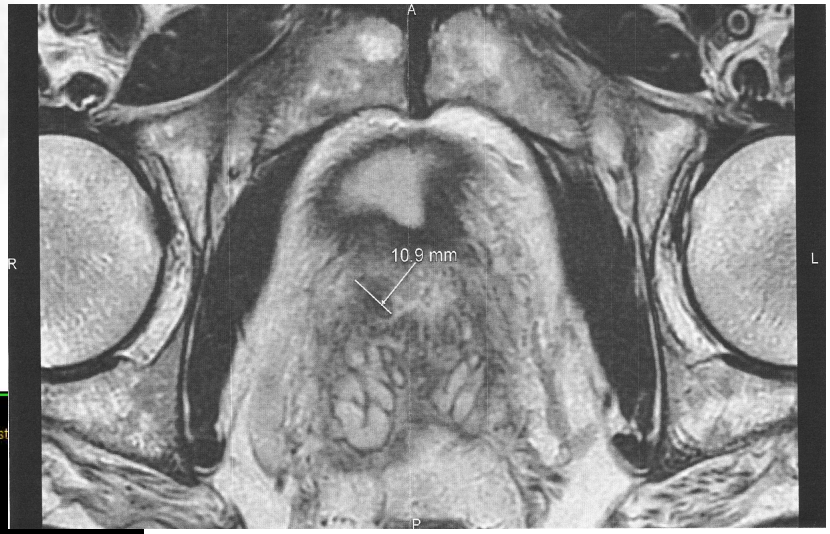
A
R
L
10.9 mm
P

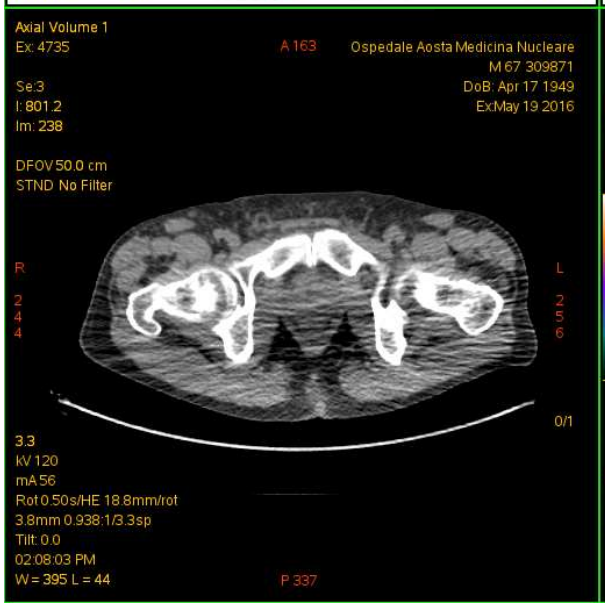
Axial Volume 1
Ex: 4735
A 163
Ospedale Aosta Medicina Nucleare
M 67 309871
Se:3
DoB: Apr 17 1949
I: 801.2
ExMay 19 2016
Im: 238
DFOV 50.0 cm
STND No Filter
R
L
2
4
4
2
5
6
0/1
3.3
kV 120
mA 56
Rot 0.50s/HE 18.8mm/rot
3.8mm 0.938:1/3.3sp
Tilt: 0.0
02:08:03 PM
W = 395 L = 44
P 337

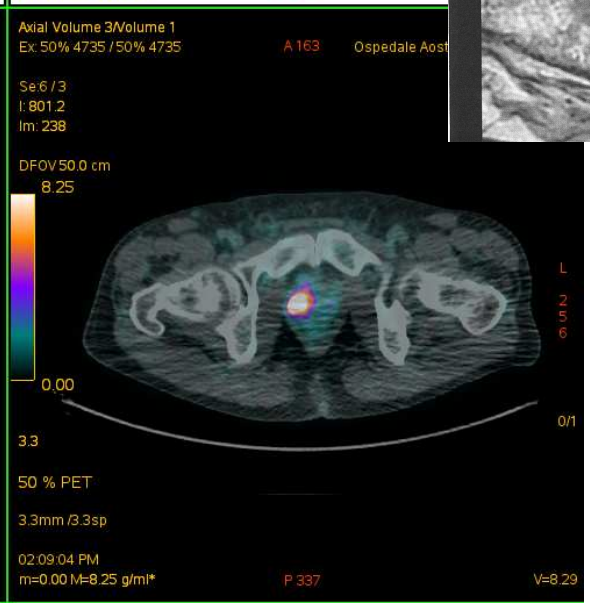
Axial Volume 3/Volume 1
Ex: 50% 4735 / 50% 4735
A 163
Ospedale Aost
Se:6 / 3
I: 801.2
Im: 238
DFOV 50.0 cm
8.25
0.00
L
2
5
6
0/1
3.3
50 % PET
3.3mm /3.3sp
02:09:04 PM
m=0.00 M=8.25 g/ml*
P 337
V=8.29

LA PET PSMA In sintesi

- Il PSMA è un promettente e specifico agente “target” per l’imaging del carcinoma della prostata

-L’imaging PET/CT con 68Ga-PSMA può fornire informazioni molecolari aggiuntive alla RM e fornire indicazioni per mirare la biopsia.

-LA PET/CT CON 68 Ga-PSMA mostra aumentata sensibilità e specificità rispetto alle metodiche di imaging standard in pazienti con tumore della prostata a intermedio e alto rischio.

-LA PET/CT CON 68 Ga-PSMA migliora la “detection rate” delle lesioni metastatiche specie per bassi valori di PSA nella recidiva biochimica di malattia-

- La migliorata “detection rate” delle lesioni può consentire di migliorare l’uso di terapie “patient tailored” e migliorare l’outcome dei pazienti.